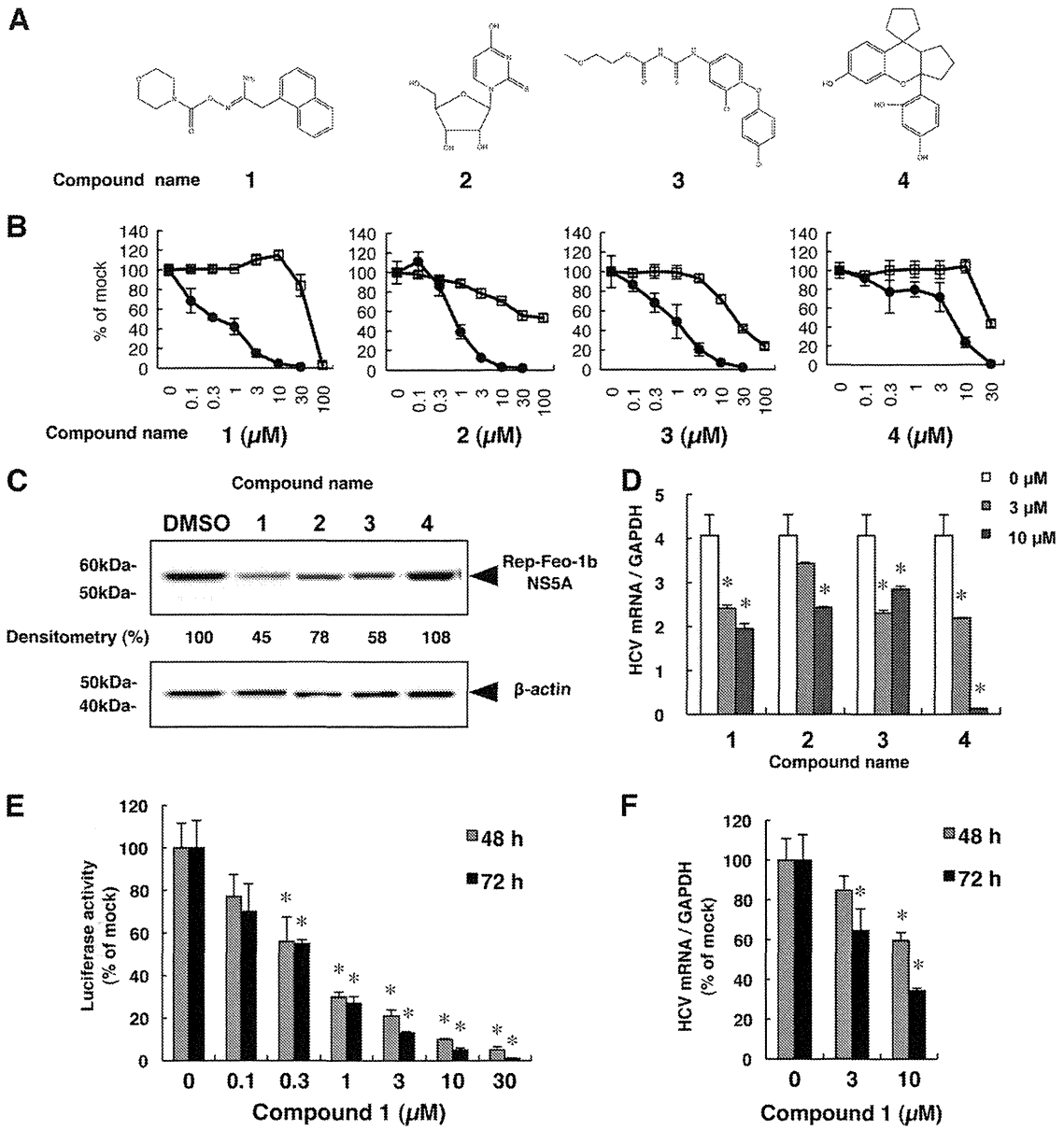

FIG 1 Effects of 4 screening hit compounds on HCV replication. (A) Chemical structures of hit compounds. (B) Huh7/Rep-Feo cells were treated with the indicated concentration of each compound for 48 h. Luciferase activities representing HCV replication are shown as percentages of the DMSO-treated control luciferase activity (solid circles). Cell viability is shown as a percentage of control viability (open squares). Each point represents the mean of triplicate data points, with the standard deviations represented as error bars. (C) Huh7/Rep-Feo cells were treated with DMSO or compounds 1 through 4 at 5 μM for 48 h, and Western blotting was performed using anti-HCV NS5A and anti-β-actin antibodies. Densitometry of NS5A protein was performed, and the results are indicated as percentages of the DMSO-treated control. The assay was repeated three times, and a representative result is shown. (D) Huh7.5.1 cells were transfected with HCV-JFH1 RNA and cultured in the presence of the indicated compounds at 3 μM or 10 μM. At 72 h after transfection, the cellular expression levels of HCV-RNA were quantified by real-time RT-PCR. The bars indicate means and SD. (E) Time-dependent reduction of luciferase activities in Huh7/Rep-Feo cells induced by compound 1. Luciferase activities are shown as percentages of the DMSO-treated control luciferase activity. The bars indicate means and SD. (F) Time-dependent reduction of cellular expression levels of HCV-RNA in HCV-JFH1-transfected cells induced by compound 1. HCV RNA levels are shown as percentages of the DMSO-treated control HCV-RNA level. The bars indicate means and SD. The asterisks indicate P values of less than 0.01.

assays, including the replicon and HCV-JFH1 virus assays. Thus, we concluded that compound 4 was an antiviral hit. These results indicated that the 4 compounds identified by cell-based screening suppressed subgenomic HCV replication and HCV replication in an HCV-based cell culture.

Hit compounds did not suppress HCV IRES-mediated translation. To determine whether the leading antiviral hits suppressed HCV IRES-dependent translation, we used the Huh7 cell line that had been stably transfected with pCIneo-Rluc IRES-Fluc. Treatment of these cells with the test compounds did not result in significant change in the internal luciferase activities at compound concentrations that suppressed expression of the HCV replicon (Fig. 2), suggesting that the effect of the hit compounds on HCV replication does not involve suppression of IRES-mediated viral-protein synthesis.

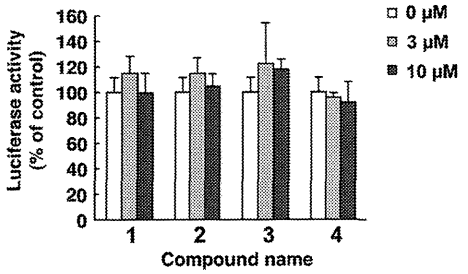

FIG 2 Hit compounds do not affect HCV IRES-mediated translation. The bicistronic reporter plasmid pC1neo-Rluc-IRES-Fluc was transfected into Huh7 cells. The cells were cultured in the presence of the indicated concentrations of compounds 1 through 4. After 6 h of treatment, luciferase activities were measured, and the values were normalized against *Renilla* luciferase activities. The assays were performed in triplicate. The bars indicate means and SD.

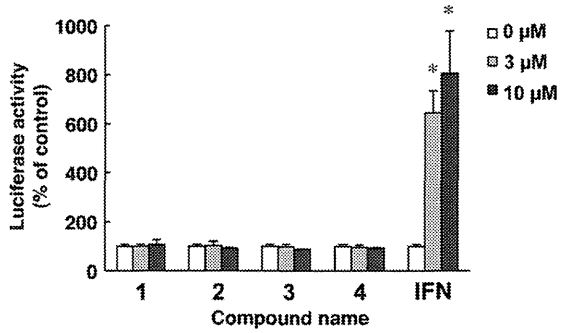

FIG 3 Hit compounds do not activate interferon-stimulated gene responses. Plasmids pISRE-TA-Luc and pRL-CMV were cotransfected into Huh7 cells. The transfected cells were cultured in the presence of the indicated concentrations of the hit compounds. After 6 h of treatment, luciferase activities were measured, and the values were normalized against *Renilla* luciferase activities. As positive controls, cells were treated with IFN-α at a concentration of 0, 3, or 10 U/ml. The bars indicate means and SD. The asterisks indicate *P* values of less than 0.01.

Hit compounds do not activate interferon-stimulated gene responses. To study whether the actions of the hit compounds involved IFN-mediated antiviral signaling that would induce expression of an IFN-stimulated gene, an ISRE-luciferase reporter plasmid, pISRE-TA-Luc, was transfected into Huh7 cells, and the transfected cells were cultured in the presence of the 4 compounds at concentrations of 0, 3, or 10 μM. In contrast to interferon, which elevated ISRE promoter activities significantly, the hit compounds showed no effects on the ISRE-luciferase activities (Fig. 3). These results indicated that the action of the hit compounds is independent of interferon signaling.

Drug synergism with IFN-α or BILN 2061. To investigate whether the hit compounds were synergistic with IFN-α or the protease inhibitor BILN 2061, we used isobologram analyses (24, 28). HCV replicon cells were treated with a combination of IFN-α or BILN 2061 and each hit compound at an EC_{50} ratio of 1:0. 4:1, 3:2, 2:3, 1:4, or 0:1, and the dose-effect results were plotted (Fig. 4A and C). The fractional EC_{50}s for IFN-α or BILN 2061 and each compound were plotted on the *x* and *y* axes, respectively, to generate an isobologram. As shown in Fig. 4B, all plots of the fractional EC_{50}s of compound 1 and IFN-α fell below the line of additivity, while the plots were located closed to the line of additivity for the treatments using IFN-α plus compound 2 or 3 and above the line for the treatment using IFN-α plus compound 4. Those results indicated that the anti-HCV effect of compound 1 was synergistic with IFN-α, the anti-HCV effects of compounds 2 and 3 were additive, and the effect of compound 4 was antagonistic. In the BILN 2061 combination study, the combination with compound 2 was slightly synergistic, while the combination with compound 1 or 3 was additive, and the combination with compound 4 was antagonistic (Fig. 4D).

SARs of compound 1 and similar compounds. We next conducted SAR analyses for hit compound 1 by screening 69 compounds with structures similar to that of compound 1 (see Table S2 in the supplemental material). Out of those compounds, we identified 4 structural analogues that suppressed subgenomic HCV replication with EC_{50}s ranging from 1.82 to 4.03 μM and SIs of 6.01 through >43.7 (Table 2 and Fig. 5A and B). Similarly, the 4 compounds designated 5, 6, 7, and 8 substantially decreased HCV-NS5A protein expression levels following treatment with the compounds (Fig. 5C). Consistent with the replicon results, the compounds significantly suppressed HCV-JFH1 mRNA in cell culture (Fig. 5D). Although the suppressive activities of the 4 compounds were similar, the original compound 1 showed the greatest anti-HCV activity. Therefore, we conducted SAR analyses of the compound 1 *N*-(morpholine-4-carbonyloxy) amidine and *N*-acyloxy-1-naphthalenacetamidine moieties. We screened 13 compounds containing *N*-(morpholine-4-carbonyloxy) amidine and 11 with *N*-acyloxy-1-naphthalenacetamidine (Fig. 6A; see Table S3 in the supplemental material). Intriguingly, 11 out of the 13 *N*-(morpholine-4-carbonyloxy) amidine compounds suppressed the subgenomic HCV replicon without cytotoxicity at a fixed concentration of 5 μM. In contrast, only 2 *N*-acyloxy-1-naphthalenacetamidine compounds decreased HCV replication (Fig. 6B and C). We also conducted dose-dependent suppression assays for HCV replicon. As shown in Table 3, 11 out of 13 *N*-(morpholine-4-carbonyloxy) amidine compounds consistently decreased subgenomic HCV replication, with EC_{50}s ranging from 1.52 through 8.62 μM and SIs of 14.2 to >61.4. Of these 11 compounds, compound 14 was the most potent, with an EC_{50} of 1.63 μM and an SI of >61.4. The antiviral effect of compound 14 against HCV-JFH1 was identical to that of the original compound 1. To identify the moiety conferring anti-HCV activity, we tested the morpholine-4-carboxyl moiety within the *N*-(morpholine-4-carboynloxy) amidine structure (Fig. 6D). Three compounds bearing the morpholine-4-carboxyl moiety were tested, and none showed suppressive activity toward the HCV replicon. These results suggested that the entire *N*-(morpholine-4-carbonyloxy) amidine moiety was important for efficient anti-HCV activity.

Effect of compound 1 on the NF-κB signaling pathway. NF-κB, composed of homo- and heterodimeric complexes of Rel-like domain-containing proteins, including p50 and p65, is a key regulator of innate and adaptive immune responses through transcriptional activation of several antiviral proteins (9, 23). We performed luciferase reporter assays, a p65 phosphorylation assay, and an IκB-α degradation assay to assess the effect of compound 1 on NF-κB signaling in host cells. Intriguingly, treatment of both Huh7 cells and HCV replicon-expressing cells with compound 1 increased NF-κB reporter activity in a dose-dependent manner (Fig. 7A and B). Consistently, treatment with compound 1 increased phosphorylated NF-κB p65 in Huh7 cells (Fig. 7C). Acti-

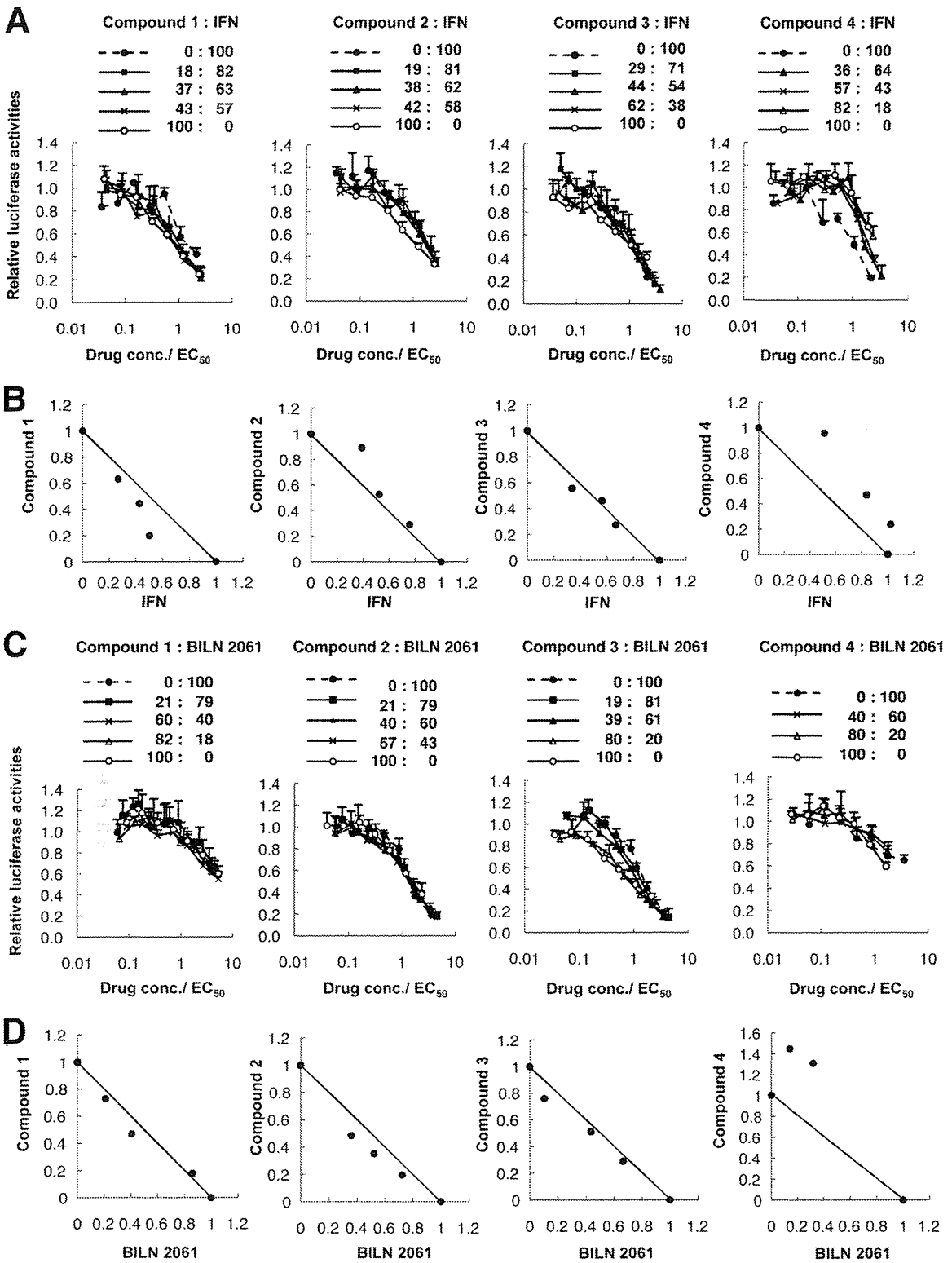

FIG 4 Drug synergism analyses: effects of each of the 4 antiviral hit compounds combined with IFN-α or BILN 2061 on HCV replication. (A and C) Huh7/Rep-Feo cells were cultured with a combination of IFN-α or BILN 2061 and antiviral hit compound 1, 2, 3, or 4 at the indicated ratios, adjusted by the EC_{50} of the individual drug. The internal luciferase activities were measured after 48 h of culture. Assays were performed in triplicate. Shown are means and SD. (B and D) Graphical presentations of isobologram analyses. For each drug combination in panels A and C, the EC_{50}s of IFN-α or BILN 2061 and compound 1, 2, 3, or 4 for inhibition of HCV replication were plotted against the fractional concentrations of IFN-α or BILN 2061 and each compound, as indicated on the x and y axis, respectively. A theoretical line of additivity is drawn between the EC_{50}s for each drug alone.

TABLE 2 Effects of derivative compounds of 1 on HCV replication[a]

Compound	EC_{50} (μM)	CC_{50} (μM)	SI
5	1.82 (0.58–5.68)	45.1 (14.3–52.5)	24.8
6	2.29 (1.57–3.34)	>100	>43.7
7	2.83 (1.43–5.78)	17.0 (5.25–38.7)	6.01
8	4.03 (3.51–4.63)	87.8 (59.1–172)	21.8

[a] The EC_{50} and CC_{50} values are reported, with 95% confidence intervals in parentheses, from a representative experiment performed in triplicate.

vation of NF-κB involves degradation of a suppressor protein, IκB-α. As shown in Fig. 7D, IκB-α protein levels were strongly decreased in cells treated with compound 1. Additionally, activation of the NF-κB pathway by TNF-α treatment significantly suppressed HCV replication (Fig. 7E). These results indicated that the antiviral action of compound 1 partially involved activation of the NF-κB signaling pathway.

DISCUSSION

Using a chimeric luciferase reporter-based subgenomic HCV-Feo replicon assay and an HCV-JFH1 cell culture, we discovered 4 novel anti-HCV compounds from cell-based screening of a library of 4,004 chemicals (Fig. 1 and Table 1). These compounds displayed anti-HCV activity at noncytotoxic concentrations. The most potent of the leading hit compounds was MCNA, and SAR analyses revealed that 4 compounds with structures similar to that of MCNA also had antiviral activity (Fig. 5). Furthermore, we showed that the *N*-(morpholine-4-carbonyloxy) amidine moiety within the structure of MCNA is essential for antiviral activity (Fig. 6).

After the development of the HCV replicon system, the study of HCV replication and discovery of novel anti-HCV agents have shown great progress. To date, our group and others have already made several successful attempts to discover novel inhibitors of HCV replication. Using Huh7/Rep-Feo cells, we previously identified novel anti-HCV substances, including cyclosporins (18, 19), short interfering RNA (siRNA) (31), hydroxyl-methyl-glutaryl coenzyme A reductase inhibitors (10), and epoxide compounds (20). Huh7/Rep-Feo cells were also used for screening a whole-genome siRNA library and successfully identified human genes that support HCV replication (27). Although the HCV replicon system cannot screen for inhibitors of viral entry and release, it is still a useful tool for rapid, reliable, and reproducible high-throughput screening. In our study, we used library sets of compounds that had probably not been used for anti-HCV drug screening before.

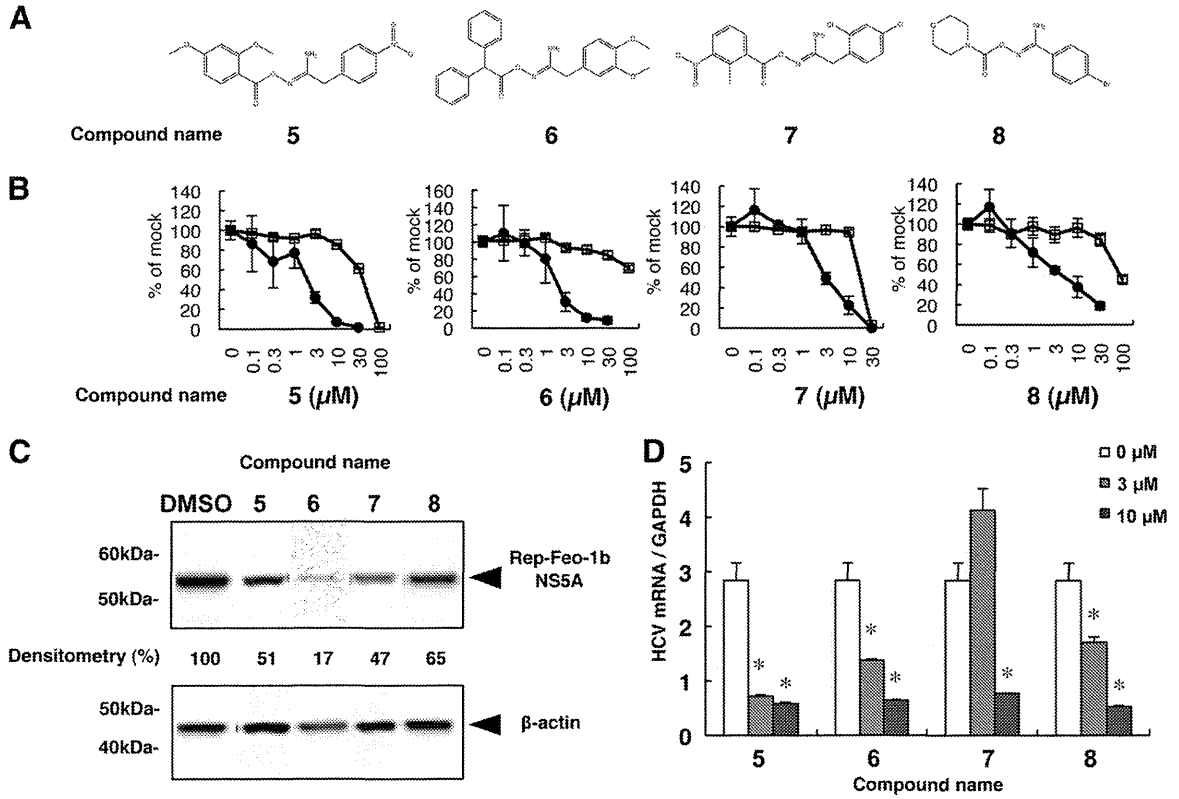

FIG 5 Effects of derivatives of compound 1 on HCV replication. (A) Chemical structures of screening hits of compound 1 derivatives. (B) Huh7/Rep-Feo cells were treated with various concentrations of each compound for 48 h. Luciferase activity for HCV RNA replication is shown as a percentage of the DMSO-treated control luciferase activity (solid circles). Cell viability is also shown as a percentage of control viability (open squares). Each point represents the mean of triplicate data points, with standard deviations represented as error bars. (C) HCV NS5A protein expression levels in Huh7/Rep-Feo cells after treatment with the hit compounds. Huh7/Rep-Feo cells were treated with DMSO and derivative compounds at 5 μM for 48 h, and Western blotting was performed using anti-HCV NS5A and anti-β-actin antibodies. Densitometry of the NS5A protein was performed, and the results are indicated as percentages of the DMSO-treated control. The assay was repeated three times, and a representative result is shown. (D) Huh7.5.1 cells were transfected with HCV-JFH1 RNA and cultured in the presence of the indicated compounds at a concentration of 3 μM or 10 μM. At 72 h after transfection, total cellular RNA was extracted, followed by real-time RT-PCR. The bars indicate means and SD. The asterisks indicate *P* values of less than 0.01. GAPDH, glyceraldehyde-3-phosphate dehydrogenase.

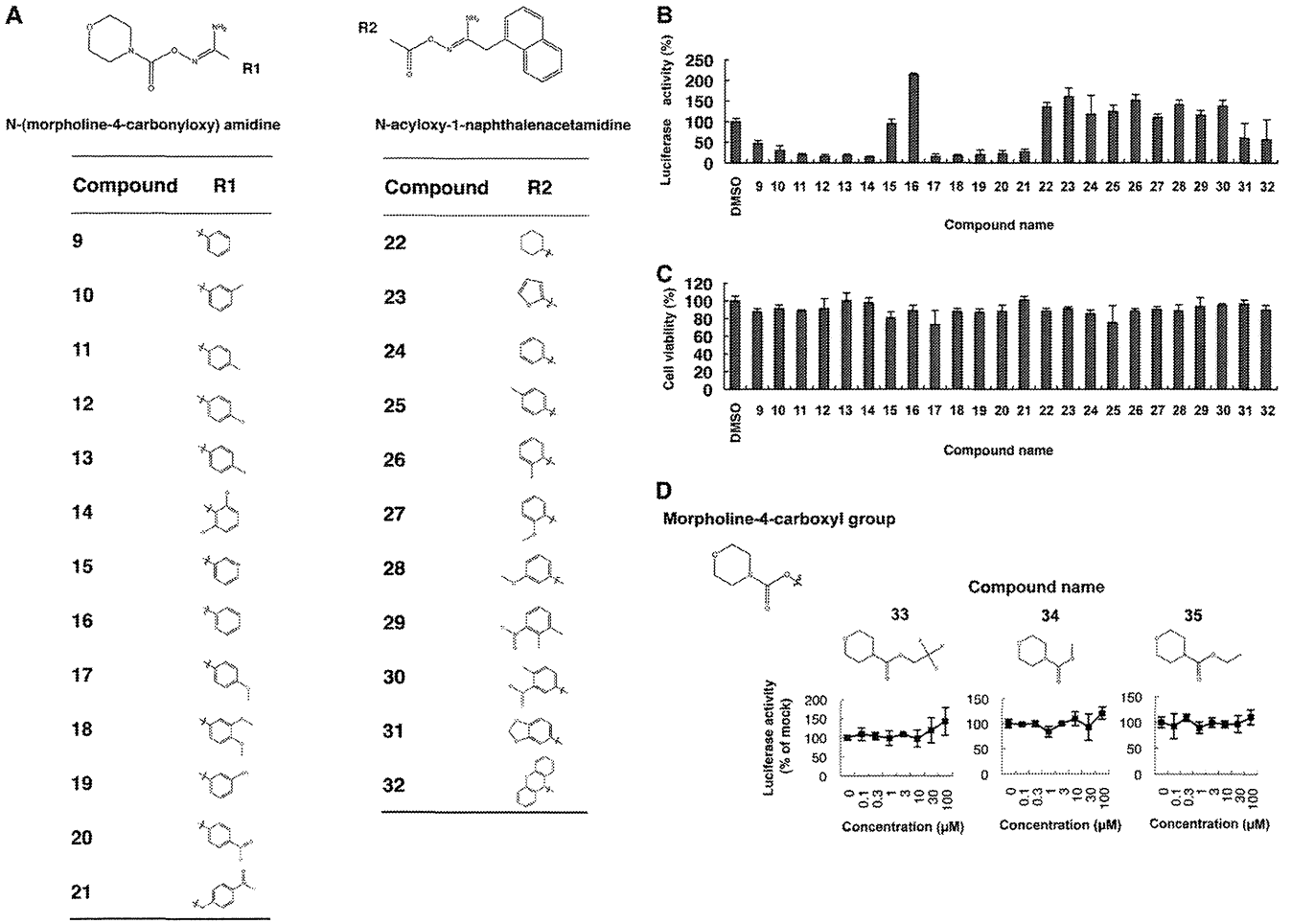

FIG 6 SARs of derivatives of compound 1 that contain *N*-(morpholine-4-carbonyloxy) amidine or *N*-acyloxy-1-naphthalenacetamidine moieties. (A) Chemical structures of compounds with *N*-(morpholine-4-carbonyloxy) amidine or *N*-acyloxy-1-naphthalenacetamidine analyzed for SARs. (B) Huh7/Rep-Feo cells were cultured in the presence of 13 compounds with *N*-(morpholine-4-carbonyloxy) amidine and 11 compounds with *N*-acyloxy-1-naphthalenacetamidine at a fixed concentration of 5 μM. The internal luciferase activities were measured after 48 h of culture. Luciferase activity for HCV RNA replication levels is shown as a percentage of the drug-negative (DMSO) control. Assays were performed in triplicate. The bars indicate means and SDs. (C) Cell viability is shown as a percentage of control viability. Assays were performed in triplicate. The bars indicate means and SD. (D) Effects of morpholine-4-carboxyl compounds on HCV replication. Huh7/Rep-Feo cells were treated with various concentrations of compound 33, 34, or 35 for 48 h. Luciferase activity for HCV RNA replication levels is shown as a percentage of the drug-negative (DMSO) control. Each point represents the mean of triplicate data points, with standard deviations represented as error bars.

TABLE 3 Effects of *N*-(morpholine-4-carbonyloxy) amidine compounds on HCV replication[a]

Compound	EC_{50} (μM)	CC_{50} (μM)	SI
9	8.62 (7.03–10.6)	>100	>11.1
10	3.32 (2.28–4.84)	47.0 (15.7–76.4)	14.2
11	1.55 (1.04–2.30)	48.8 (12.8–95.6)	31.5
12	1.52 (1.14–2.02)	51.0 (16.2–96.7)	33.6
13	1.60 (1.36–1.88)	38.6 (29.4–50.7)	24.1
14	1.63 (1.34–2.00)	>100	>61.4
15	ND	ND	ND
16	ND	ND	ND
17	1.77 (1.39–2.26)	63.3 (21.8–128)	35.8
18	3.80 (2.48–5.83)	100 (86.8–138)	26.3
19	1.99 (1.59–2.48)	55.1 (14.8–105)	27.7
20	2.61 (1.68–4.05)	>100	>38.3
21	1.55 (1.45–1.67)	94.6 (93.0–98.0)	61.0

[a] The EC_{50} and CC_{50} values are reported, with 95% confidence intervals in parentheses, from a representative experiment performed in triplicate. ND, not determined.

The morpholine moiety is a common pharmacophore present in many biosynthetic compounds, such as antimycotic agents (4, 21), and inhibitors of phosphoinositide 3-kinases (5, 16, 30), TNF-α-converting enzymes (14), and matrix metalloproteinases (1). Among the antimycotic morpholine derivatives, amorolfine has been widely used to treat onychomycosis (4, 21). The morpholino oxygen in a synthetic phosphoinositide 3-kinase inhibitor, LY294002, participated directly in a key hydrogen-bonding interaction at the ATP-binding site of phosphoinositide 3-kinase γ (30). Although the morpholine moieties are key components of many inhibitors, anti-HCV morpholine compounds have not yet been reported. In this report, we demonstrated for the first time that a morpholine-bearing compound, *N*-(morpholine-4-carbonyloxy) amidine, had a potent antiviral effect on HCV replication.

Among the 4 hit compounds, MCNA activated the NF-κB pathway (Fig. 7A, B, C, and D). NF-κB is a central regulator of innate and adaptive immune responses. NF-κB-induced tran-

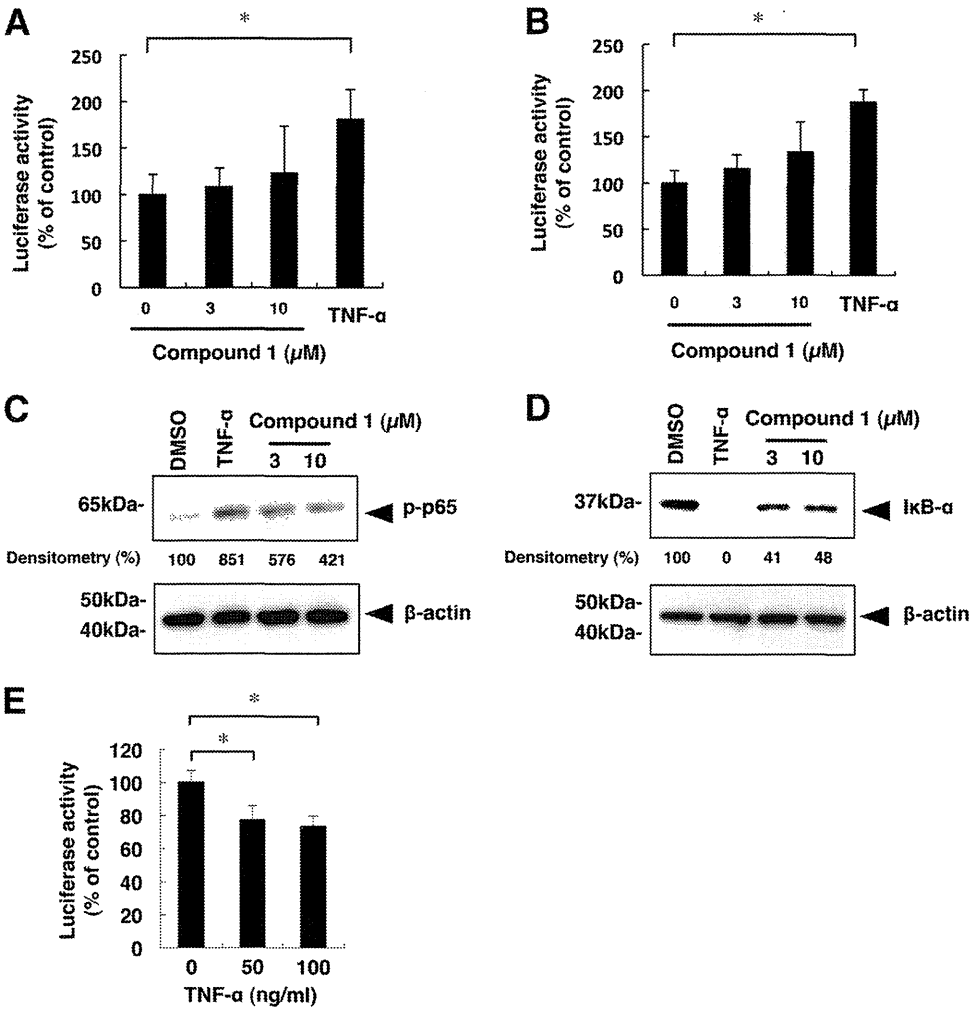

FIG 7 Effects of compound 1 on the NF-κB signaling pathway. (A and B) NF-κB-responsive luciferase reporter assays. The plasmids pNF-κB-TA-Fluc and pRL-CMV were cotransfected into Huh7 cells (A) or HCV replicon-expressing cells (B). At 24 h after transfection, cells were treated with compound 1 at a concentration of 0, 3, or 10 μM. After 6 h, luciferase activities were measured, and the values were normalized against *Renilla* luciferase activities. As a positive control, cells were treated with TNF-α (50 ng/ml). Assays were performed in triplicate. The bars indicate means and SD. (C and D) Huh7 cells were treated for 30 min with compound 1 at concentrations of 3 and 10 μM, and Western blot analyses of phosphorylated p65 and IκBα were conducted. As a positive control, cells were treated with TNF-α (50 ng/ml). β-Actin served as a loading control. Densitometry of phosphorylated p65 protein and IκB-α protein was performed, and the results are indicated as percentages of the DMSO-treated control. The assay was repeated three times, and a representative result is shown. (E) Effect of activation of NF-κB signaling on HCV RNA replication. Huh7/Rep-Feo cells were treated with TNF-α at a concentration of 0, 50, or 100 ng/ml for 48 h. Luciferase activity for HCV RNA replication levels is shown as a percentage of untreated negative-control luciferase activity. Assays were performed in replicates of 6. The asterisks indicate *P* values of less than 0.01.

scription is induced in response to a variety of signals, including proinflammatory cytokines, stress induction, and by-products of microbial and viral infection (9). In HCV-infected cells, activation of transcription factors, such as NF-κB and many interferon regulatory factors, proceeds mainly through Toll-like receptors and RIG-I-dependent host signaling pathways triggered by double-stranded RNA products (3). NF-κB, interferon regulatory factor 1, and interferon regulatory factor 3 bind to the positive regulatory domains of the IFN-β promoter to induce IFN-β expression and elicit antiviral states in host cells (23). Therefore, we hypothesized that the augmentation of host antiviral response through NF-κB activation is an important strategy for anti-HCV treatment. Our demonstration that the activation of NF-κB signaling suppressed HCV replication appears to follow this strategy (Fig. 7E). In support of the idea, Toll-like receptor 7 agonist has shown anti-HCV effects in a preclinical study (7). The anti-HCV activities of MCNA cannot be explained solely by NF-κB activation, because its antiviral activity was much more potent than selective NF-κB activation by TNF-α treatment (Fig. 7E). There remains the possibility that MCNA has a direct viral target. It will be important to assess whether long-term exposure to the compounds could select resistant variants. Although other mechanisms may underlie the antiviral activity, we hypothesize that one of the antiviral mechanisms of MCNA is NF-κB activation that is independent of IFN signaling.

Although several DAAs are currently in advanced clinical trials and the recently approved telaprevir and boceprevir combination therapies achieved high sustained virologic response rates, the frequent emergence of drug-resistant viruses is a major weakness of such agents. An ongoing search for more potent

and less toxic antiviral agents to improve anti-HCV chemotherapeutics is necessary. Our results indicate that MCNA and related *N*-(morpholine-4-carbonyloxy) amidine compounds constitute a new class of anti-HCV agents. Additional investigations elucidating their mechanism of action, and future modifications to improve anti-HCV activity, may open a new anti-HCV therapeutic window.

ACKNOWLEDGMENTS

We thank Frank Chisari for providing Huh7.5.1 cells, Takaji Wakita for providing the plasmid pJFH1full, and the Chemical Biology Screening Center of Tokyo Medical and Dental University for their assistance in this work.

This study was supported in part by grants from the Ministry of Education, Culture, Sports, Science and Technology of Japan; the Japan Society for the Promotion of Science, Ministry of Health, Labor and Welfare; the Japan Health Sciences Foundation; and the National Institute of Biomedical Innovation.

We declare that we have nothing to disclose regarding funding from industries or conflicts of interest with respect to the manuscript.

REFERENCES

1. **Almstead NG, et al.** 1999. Design, synthesis, and biological evaluation of potent thiazine- and thiazepine-based matrix metalloproteinase inhibitors. J. Med. Chem. **42**:4547–4562.
2. **Bailey M, Williams NA, Wilson AD, Stokes CR.** 1992. PROBIT: weighted probit regression analysis for estimation of biological activity. J. Immunol. Methods **153**:261–262.
3. **Bigger CB, et al.** 2004. Intrahepatic gene expression during chronic hepatitis C virus infection in chimpanzees. J. Virol. **78**:13779–13792.
4. **Flagothier C, Piérard-Franchimont C, Piérard GE.** 2005. New insights into the effect of amorolfine nail lacquer. Mycoses **48**:91–94.
5. **Hickson I, et al.** 2004. Identification and characterization of a novel and specific inhibitor of the ataxia-telangiectasia mutated kinase ATM. Cancer Res. **64**:9152–9159.
6. **Hoofnagle JH, Seeff LB.** 2006. Peginterferon and ribavirin for chronic hepatitis C. N. Engl. J. Med. **355**:2444–2451.
7. **Horsmans Y, et al.** 2005. Isatoribine, an agonist of TLR7, reduces plasma virus concentration in chronic hepatitis C infection. Hepatology **42**:724–731.
8. **Kanazawa N, et al.** 2004. Regulation of hepatitis C virus replication by interferon regulatory factor 1. J. Virol. **78**:9713–9720.
9. **Karin M, Lin A.** 2002. NF-kappaB at the crossroads of life and death. Nat. Immunol. **3**:221–227.
10. **Kim SS, et al.** 2007. A cell-based, high-throughput screen for small molecule regulators of hepatitis C virus replication. Gastroenterology **132**: 311–320.
11. **Kwo PY, et al.** 2010. Efficacy of boceprevir, an NS3 protease inhibitor, in combination with peginterferon alfa-2b and ribavirin in treatment-naive patients with genotype 1 hepatitis C infection (SPRINT-1): an open-label, randomised, multicentre phase 2 trial. Lancet **376**:705–716.
12. **Kwong AD, Kauffman RS, Hurter P, Mueller P.** 2011. Discovery and development of telaprevir: an NS3-4A protease inhibitor for treating genotype 1 chronic hepatitis C virus. Nat. Biotechnol. **29**:993–1003.
13. **Lauer GM, Walker BD.** 2001. Hepatitis C virus infection. N. Engl. J. Med. **345**:41–52.
14. **Levin JI, et al.** 2005. Acetylenic TACE inhibitors. Part 2: SAR of six-membered cyclic sulfonamide hydroxamates. Bioorg. Med. Chem. Lett. **15**:4345–4349.
15. **Lipinski CA, Lombardo F, Dominy BW, Feeney PJ.** 2001. Experimental and computational approaches to estimate solubility and permeability in drug discovery and development settings. Adv. Drug Deliv. Rev. **46**:3–26.
16. **Menear KA, et al.** 2009. Identification and optimisation of novel and selective small molecular weight kinase inhibitors of mTOR. Bioorg. Med. Chem. Lett. **19**:5898–5901.
17. **Mishima K, et al.** 2010. Cell culture and in vivo analyses of cytopathic hepatitis C virus mutants. Virology **405**:361–369.
18. **Nakagawa M, et al.** 2004. Specific inhibition of hepatitis C virus replication by cyclosporin A. Biochem. Biophys. Res. Commun. **313**:42–47.
19. **Nakagawa M, et al.** 2005. Suppression of hepatitis C virus replication by cyclosporin A is mediated by blockade of cyclophilins. Gastroenterology **129**:1031–1041.
20. **Peng LF, et al.** 2007. Identification of novel epoxide inhibitors of hepatitis C virus replication using a high-throughput screen. Antimicrob. Agents Chemother. **51**:3756–3759.
21. **Polak A, Jäckel A, Noack A, Kappe R.** 2004. Agar sublimation test for the in vitro determination of the antifungal activity of morpholine derivatives. Mycoses **47**:184–192.
22. **Poordad F, et al.** 2011. Boceprevir for untreated chronic HCV genotype 1 infection. N. Engl. J. Med. **364**:1195–1206.
23. **Randall RE, Goodbourn S.** 2008. Interferons and viruses: an interplay between induction, signalling, antiviral responses and virus countermeasures. J. Gen. Virol. **89**:1–47.
24. **Sakamoto N, et al.** 2007. Bone morphogenetic protein-7 and interferon-alpha synergistically suppress hepatitis C virus replicon. Biochem. Biophys. Res. Commun. **357**:467–473.
25. **Sarrazin C, Zeuzem S.** 2010. Resistance to direct antiviral agents in patients with hepatitis C virus infection. Gastroenterology **138**:447–462.
26. **Soothill JS, Ward R, Girling AJ.** 1992. The IC50: an exactly defined measure of antibiotic sensitivity. J. Antimicrob. Chemother. **29**:137–139.
27. **Tai AW, et al.** 2009. A functional genomic screen identifies cellular cofactors of hepatitis C virus replication. Cell Host Microbe **5**:298–307.
28. **Tanabe Y, et al.** 2004. Synergistic inhibition of intracellular hepatitis C virus replication by combination of ribavirin and interferon-alpha. J. Infect. Dis. **189**:1129–1139.
29. **Wakita T, et al.** 2005. Production of infectious hepatitis C virus in tissue culture from a cloned viral genome. Nat. Med. **11**:791–796.
30. **Walker EH, et al.** 2000. Structural determinants of phosphoinositide 3-kinase inhibition by wortmannin, LY294002, quercetin, myricetin, and staurosporine. Mol. Cell **6**:909–919.
31. **Yokota T, et al.** 2003. Inhibition of intracellular hepatitis C virus replication by synthetic and vector-derived small interfering RNAs. EMBO Rep. **4**:602–608.
32. **Zhong J, et al.** 2005. Robust hepatitis C virus infection in vitro. Proc. Natl. Acad. Sci. U. S. A. **102**:9294–9299.

AAC
Journals.ASM.org

ENT1, a Ribavirin Transporter, Plays a Pivotal Role in Antiviral Efficacy of Ribavirin in a Hepatitis C Virus Replication Cell System

Minami Iikura,[a] Tomomi Furihata,[a] Misa Mizuguchi,[a] Miki Nagai,[a] Masanori Ikeda,[b] Nobuyuki Kato,[b] Akihito Tsubota,[c] and Kan Chiba[a]

Laboratory of Pharmacology and Toxicology, Graduate School of Pharmaceutical Sciences, Chiba University, Chiba, Japan[a]; Department of Tumor Virology, Okayama University Graduate School of Medicine, Dentistry, and Pharmaceutical Science, Okayama, Japan[b]; and Institute of Clinical Medicine and Research, Jikei University School of Medicine, Chiba, Japan[c]

We previously showed that equilibrative nucleoside transporter 1 (ENT1) is a primary ribavirin transporter in human hepatocytes. However, because the role of this transporter in the antiviral mechanism of the drug remains unclear, the present study aimed to elucidate the role of ENT1 in ribavirin antiviral action. OR6 cells, a hepatitis C virus (HCV) replication system, were used to evaluate both ribavirin uptake and efficacy. The ribavirin transporter in OR6 cells was identified by mRNA expression analyses and transport assays. Nitrobenzylmercaptopurine riboside (NBMPR) and micro-RNA targeted to ENT1 mRNA (miR-ENT1) were used to reduce the ribavirin uptake level in OR6 cells. Our results showed that ribavirin antiviral activity was associated with its accumulation in OR6 cells, which was also closely associated with the uptake of the drug. It was found that the primary ribavirin transporter in OR6 cells was ENT1 and that inhibition of ENT1-mediated ribavirin uptake by NBMPR significantly attenuated the antiviral activity of the drug as well as its accumulation in OR6 cells. The results also showed that even a small reduction in the ENT1-mediated ribavirin uptake, achieved in this case using miR-ENT1, caused a significant decrease in its antiviral activity, thus indicating that the ENT1-mediated ribavirin uptake level determined its antiviral activity level in OR6 cells. In conclusion, our results show that by facilitating its uptake and accumulation in OR6 cells, ENT1 plays a pivotal role in the antiviral effectiveness of ribavirin and therefore provides an important insight into the efficacy of the drug in anti-HCV therapy.

Chronic hepatitis C is a major cause of liver cirrhosis and hepatocellular carcinoma, and a combination of interferon-α (IFN-α) and ribavirin is a standard anti-hepatitis C virus (HCV) therapy. Since the addition of ribavirin to IFN-α significantly improves the rate of sustained virologic response (SVR) (40 to 60% in genotype 1 patients) (5), the drug plays a key role in current anti-HCV therapy.

Ribavirin, a purine nucleoside analog, is phosphorylated intracellularly to form mono-, di-, and tri-phosphates, which then accumulate within cells at high concentrations (4, 13). While the primary anti-HCV mechanisms of the drug are still under debate, it is considered likely that the important actions take place within the cells themselves, and several mechanisms have been proposed to explain what occurs there. These include inhibition of inosine monophosphate dehydrogenase (reviewed in references 4 and 7 and references therein). Additionally, a recent study revealed that ribavirin potentiates IFN-α action by augmenting IFN-stimulated induction of gene expression (16).

Taking into consideration the above-mentioned mechanisms, it is reasonable to assume that the uptake of ribavirin into hepatocytes is a prerequisite for its antiviral activity. Since ribavirin is a hydrophilic molecule, import of the drug into cells requires host nucleoside transporters, which are divided into two families: equilibrative nucleoside transporters (such as ENT1 to ENT4) and concentrative nucleoside transporters (such as CNT1 to CNT3) (9). ENTs are facilitated transporters, while CNTs are sodium-dependent active transporters. These transporters differ in tissue distribution, substrate preference, and inhibitor sensitivity. For example, sensitivities to inhibition by nitrobenzylmercaptopurine riboside (NBMPR) are different between ENT1 and ENT2 (20).

Our recent investigations into the ribavirin uptake system in human hepatocytes determined that ENT1 is a primary ribavirin uptake transporter (6). In addition, Morello et al. (12) reported the association of an intronic single nucleotide polymorphism (SNP) of the *SLC29A1* (ENT1) gene with rapid virologic response (RVR; defined as an undetectable serum HCV RNA level at week 4) of treatment of genotype-1 Caucasian patients. More recently, Tsubota and colleagues revealed that another intronic SNP in the *SLC29A1* gene is associated with SVR, as well as RVR, in genotype-1 Japanese patients (18). Based on these findings, it can be hypothesized that ENT1 plays an essential role in ribavirin anti-HCV activity.

In the present study, along with a detailed characterization of ribavirin uptake and its relationship to antiviral activity, we tested the above-mentioned hypothesis through the use of OR6 cells, which have been established as an efficient replication system for the HCV RNA genome. The HCV replication level was evaluated by monitoring the level of *Renilla* luciferase activity (8), which enabled us to simultaneously evaluate both ribavirin uptake and its antiviral activity.

MATERIALS AND METHODS

Cell culture. OR6 cells were cloned from ORN/C-5B/KE cells (derived from Huh-7 cells) supporting genome-length HCV RNA (strain O of

Received 20 September 2011 Returned for modification 24 October 2011
Accepted 27 December 2011
Published ahead of print 9 January 2012
Address correspondence to Tomomi Furihata, tomomif@faculty.chiba-u.jp.
Supplemental material for this article may be found at http://aac.asm.org/.

doi:10.1128/AAC.05762-11

genotype 1b) containing the *Renilla* luciferase reporter gene, and the cells were cultured as described previously (8). Huh-7 cells were obtained from the Institute of Development, Aging and Cancer, Tohoku University (Sendai, Japan). The Huh-7 cells were cultured at 37°C with 5% CO_2–95% air in RPMI 1640 medium (Invitrogen, Carlsbad, CA) with 10% fetal bovine serum, 50 U/ml penicillin, and 50 μg/ml streptomycin.

Luciferase reporter assay. OR6 cells were plated 1 day prior to the assay on 24-well plates at 1.5×10^4 to 2.5×10^4 cells/well, followed by treatment with ribavirin (Wako, Osaka, Japan) in the absence of G418 and at the indicated concentrations for 24, 48, and 72 h. The cells were then subjected to the luciferase assay using a dual-luciferase reporter assay system (Promega, Madison, WI) according to the manufacturer's protocol. For data normalization, the protein contents were determined with a Pierce 660-nm protein assay reagent (Thermo Fisher Scientific, Rockford, IL) according to the manufacturer's protocol. The relative luciferase activity value of the untreated or vehicle treated cells (dimethyl sulfoxide [DMSO] for NBMPR and sterile water for others) was set to 100%. NBMPR (Sigma, St. Louis, MO), hypoxanthine (MP Biomedicals, Solon, OH), and formycin B (Berry & Associates, Ann Arbor, MI) were included in inhibition analyses at various concentrations.

Western blot analysis. OR6 cells treated with ribavirin at various concentrations in the absence of G418 for 24, 48, and 72 h were harvested and homogenized. The homogenates (60 μg/well) were resolved in a sodium dodecyl sulfate (SDS)–15% polyacrylamide gel and then transferred onto a nitrocellulose membrane. The membrane was blocked with 5% skim milk and then incubated with either antibodies against the HCV core protein (2,000-fold dilution; Institute of immunology, Tokyo, Japan) or antibodies against β-actin (500-fold dilution; Sigma). Immunocomplexes were detected with enhanced chemiluminescence (ECL) Western blotting detection reagents (GE Healthcare, Giles, United Kingdom).

Accumulation assay. OR6 cells were plated 1 day prior to the assay on 24-well plates, after which the cells were incubated with 0.5 μCi/ml [^{3}H]ribavirin (Moravek Biochemicals, Brea, CA) and nonradiolabeled ribavirin at various concentrations. NBMPR was included in inhibition analyses at concentrations of 0.1, 1, 3, 10, 31, and 100 μM. After treatment for 9.6, 24, 48, or 72 h, the cells were washed twice with ice-cold Na^+-free Krebs-Henseleit buffer (KHB) and lysed with 0.2% SDS. Radioactivity was measured using a liquid scintillation counter (LSC 5100; Aloka, Tokyo, Japan). The protein contents were determined as described above. To completely inhibit ENT-mediated ribavirin uptake, 30 μM dipyridamole (Wako) was used in the same experimental sets (20). The data were calculated by subtracting the accumulation values obtained with dipyridamole from those without dipyridamole at the same ribavirin concentrations. All assays were performed at 37°C.

Transport assays. Transport assays were performed using the previously described centrifugal filtration method (6). OR6 cells were collected and resuspended in ice-cold Na^+-containing KHB or Na^+-free KHB at 1.4×10^6 cells/ml. NBMPR, troglitazone (Wako), hypoxanthine, and formycin B were included in the inhibition analyses. Since the rate of ribavirin uptake by OR6 cells was linear for at least 60 s in the preliminary assays, the incubation time was set to 30 s. The radioactivity and protein contents of the cells used in the assay were measured as described above. The same experiments were also performed at 4°C, and the data were obtained by subtracting the uptake levels at 4°C from those at 37°C at the same ribavirin concentrations.

Total RNA preparation, cDNA synthesis, reverse transcription-PCR (RT-PCR), and quantitative real-time PCR (qPCR). Total RNA preparation, cDNA synthesis, RT-PCR, and qPCR were performed using previously described procedures (6). Among the nucleoside transporters, ENT1, ENT2, CNT2, and CNT3 mRNAs were examined by RT-PCR because they have been identified as ribavirin transporters (21). The primers for RT-PCR and qPCR are listed in Table S1 in the supplemental material. The UPL universal probes used were no. 9 (ENT1), no. 48 (ENT2), and no. 60 (glyceraldehyde 3-phosphate dehydrogenase [GAPDH]).

Knockdown of ENT1 mRNA expression in OR6 cells. The BLOCK-iT Pol II miR RNAi expression vector kit (Invitrogen) was used to suppress ENT1 mRNA expression in OR6 cells. The oligonucleotide containing micro-RNA targeted to ENT1 mRNA (miR-ENT1) was cloned into the pcDNA6.2-GW/EmGFP-miR vector. The control plasmid pcDNA6.2-GW/EmGFP-miR-neg, carrying an insert that is not known to target any identified vertebrate genes (miR-Neg), was used as a negative control. The sequences of inserts are shown in Table S1 in the supplemental material. The plasmids were transfected into OR6 cells using Lipofectamine LTX (Invitrogen). Two days after transfection, the culture medium was replaced with fresh medium containing 4 μg/ml blasticidin to obtain cells stably expressing miR-ENT1 (OR6/miR-ENT1) and cells stably expressing miR-Neg (OR6/miR-Ng).

Data analysis. Statistical analysis was performed using Student's *t* test. The four-parameter logistic model was used to calculate the 50% effective concentration (EC_{50}).

RESULTS

Concentration- and time-dependent anti-HCV activity and accumulation of ribavirin in OR6 cells. The inhibitory effects of ribavirin (1 to 3,162 μM) on HCV replication in OR6 cells were analyzed by monitoring the luciferase activity and HCV core protein expression levels. It was found that the HCV replication activity and core protein levels decreased in a ribavirin concentration-dependent manner (Fig. 1A and B), while the level of ribavirin accumulation increased in a saturable manner (Fig. 1C). Next, the time course of anti-HCV activity of ribavirin at concentrations of 10, 100, and 1,000 μM was examined. The results of our examination showed that, similar to the concentration-dependent profile, the HCV replication activity and core protein amounts decreased over time at each of the ribavirin concentrations tested (Fig. 1D and E) and that the levels of ribavirin accumulation increased linearly or saturably over time (Fig. 1F). These results suggest that ribavirin exerts concentration- and time-dependent antiviral activity that could be associated with the concentration- and time-dependent intracellular accumulation of the drug.

Identification of the ribavirin uptake transporter in OR6 cells. To identify the ribavirin uptake transporter in OR6 cells, we characterized the uptake profile of the drug and the nucleoside transporters mRNA expression in the cells. The ribavirin (1 to 3,162 μM) uptake level in Na^+-plus KHB was found to increase linearly up to 3 mM (Fig. 2A), and the uptake activities of the drug (nmol/mg protein/30 s) at 10, 100 (data not shown), and 1,000 μM were recorded as 0.03 ± 0.01, 0.33 ± 0.02 and 3.2 ± 0.3, respectively (Fig. 2B). The removal of Na^+ from the transport medium did not affect the uptake activities at any of the ribavirin concentrations tested, indicating that all the uptake activities of the drug were sodium independent. These activities were mostly abolished by the addition of 100 μM NBMPR, an inhibitor of ENT1 and ENT2. Consistently, the results of RT-PCR showed that ENT1 and ENT2 mRNAs were abundantly expressed in OR6 cells, while hardly any CNT2 and CNT3 mRNAs were expressed (Fig. 2C). During the above-described experiments, we found that a low concentration of NBMPR (100 nM) failed to inhibit ribavirin uptake by OR6 cells (M. Iikura, unpublished data). Considering that ENT1-mediated nucleoside uptake is generally sensitive to NBMPR inhibition at 100 nM (20), it was hypothesized that ENT2 should have contributed to ribavirin uptake in OR6 cells. However, our previous results indicated that ENT2 cannot transport ribavirin (6). Therefore, to clearly distinguish between ENT1- and

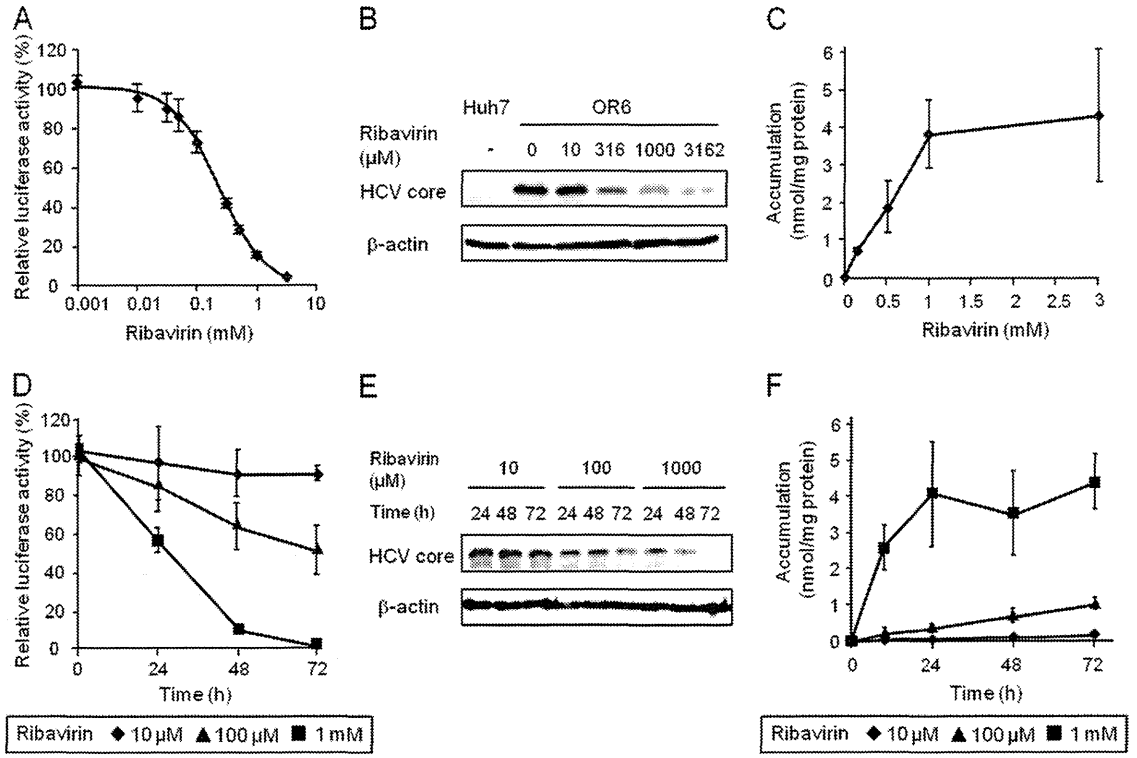

FIG 1 Concentration- and time-dependent profiles of anti-HCV activity and accumulation of ribavirin in OR6 cells. (A) OR6 cells were treated with ribavirin at concentrations of 0, 1, 10, 31, 50, 100, 316, 500, 1,000 and 3,162 μM for 48 h. The value of relative luciferase activity in the absence of ribavirin was set to 100%. (B) Expression levels of HCV core protein in OR6 cells treated with ribavirin for 48 h were examined by Western blot analysis. β-Actin was used as a loading control. Huh-7 cells were used as a negative control. (C) OR6 cells were treated with ribavirin at concentrations of 0.1, 0.5, 1, and 3 mM for 48 h, after which the radioactivity within the cells was determined. (D) OR6 cells were treated with ribavirin. The value of relative luciferase activity in the absence of ribavirin at each time point was set to 100%. (E) Expression levels of HCV core protein in OR6 cells treated with ribavirin were examined by Western blot analysis. (F) OR6 cells were treated with ribavirin, after which the radioactivity within the cells was determined. Values are means and standard deviations (SD) of the relative luciferase activity or the accumulation for three independent experiments. Each experiment was performed in duplicate. For Western blotting, the representative result for three independent assays was shown.

ENT2-mediated ribavirin uptake, inhibition analysis was performed using troglitazone (60 μM), hypoxanthine (5 mM), and formycin B (50 μM). Troglitazone has been reported to specifically inhibit ENT1 activity (10). Hypoxanthine and formycin B, at the indicated concentrations, were previously reported to preferentially inhibit ENT2 activity (3, 22), and we confirmed the inhibitory effects of these compounds on ENT2 activity by using HeLa cells (see Fig. S1 in the supplemental material). The results of the inhibition analysis showed that troglitazone completely inhibited the ribavirin uptake activity, while neither hypoxanthine nor formycin B inhibited uptake of the drug in OR6 cells (Fig. 2D). Taken together, the results indicated that, even though the affinity of ENT1 of OR6 cells for NBMPR was somehow reduced, ENT1 was exclusively responsible for the ribavirin uptake in OR6 cells.

Effect of inhibition of ribavirin uptake on its anti-HCV activity. After it was determined that ENT1 was responsible for ribavirin uptake in OR6 cells, the role of ENT1 in the anti-HCV activity of the drug (100 μM and 1 mM) was examined by chemical inhibition of ENT1-mediated ribavirin uptake in OR6 cells. Since troglitazone itself somewhat repressed HCV replication in OR6 cells (Iikura, unpublished), NBMPR was used as an ENT1 inhibitor. As shown in Fig. 3A, NBMPR decreased the level of ribavirin uptake in a dose-dependent manner and, accordingly, decreased the accumulation level of the drug in a dose-dependent manner (Fig. 3B). In association with these decreases, it was determined that the ribavirin antiviral effect was weakened by NBMPR in a concentration-dependent manner (Fig. 3C). We confirmed that ENT1 protein expression was not changed in the cells treated with the highest ribavirin and NBMPR concentrations for 48 h (see Fig. S2 in the supplemental material). To further clarify the importance of ENT1-mediated ribavirin uptake in its antiviral effects, the concentration and time dependencies of the antiviral effects of the drug were examined in cells treated with NBMPR or its vehicle (0.1% DMSO). The concentration of NBMPR was set to 7 μM, which is near the EC_{50} against ENT1 activity calculated from the results of Fig. 3A, indicating that the ENT1 activity level of NBMPR-treated cells was approximately half that of the vehicle-treated cells. As shown in Fig. 3D, the EC_{50} of ribavirin in the NBMPR-treated cells was 399 $\pm$ 22 μM, which was significantly higher than that of the vehicle-treated cells (203 $\pm$ 47 μM, P = 0.0005) (The results of the individual experiments are shown in Fig. S3 in the supplemental material.) In addition, the response to ribavirin in the NBMPR-treated cells was significantly delayed in comparison to that in the vehicle-treated cells (Fig. 3E). We also examined the constraining effects of ENT2 inhibitors on ribavirin antiviral activity but found that hypoxanthine (5 mM) and formycin B (50 μM) had no effect (see Fig. S4 in the supplemental material). Furthermore, NBMPR, hypoxanthine and formycin B

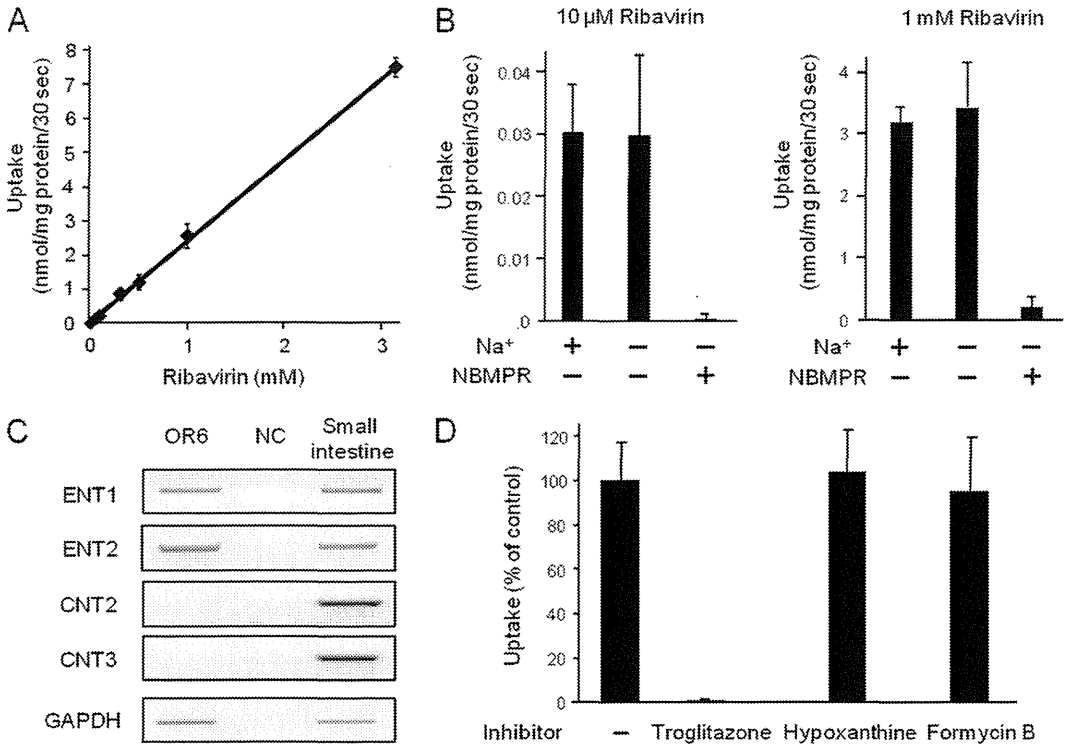

FIG 2 Identification of the ribavirin uptake transporter in OR6 cells. (A) The concentration dependence of ribavirin uptake (concentrations are given in the legend to Fig. 1A) by OR6 cells was analyzed in Na^+-containing KHB. (B) Ribavirin uptake by OR6 cells was analyzed in Na^+-containing KHB and Na^+-free KHB. In inhibition assays, the effect of 100 μM NBMPR on ribavirin uptake was analyzed in Na^+-free KHB. (C) ENT1, ENT2, CNT2, CNT3 and GAPDH mRNA expression was examined by RT-PCR. Small intestine cDNA was used as a PCR control. NC, nontemplate control. Representative results from one of three independent analyses are shown. (D) To clearly distinguish between ENT1- and ENT2-mediated ribavirin uptake, inhibition analysis of ribavirin (100 μM) uptake by OR6 cells was performed in Na^+-free KHB in the absence of inhibitor (−) or the presence of troglitazone (ENT1 inhibitor, 60 μM), hypoxanthine (ENT2 inhibitor, 5 mM), or formycin B (ENT2 inhibitor, 50 μM). The value of the transport activity of the control (no inhibitor) was set to 100%. In the above-described experiments, each value is the mean plus SD from three independent experiments, each performed in duplicate.

were found to have no effect on HCV replication activity in the above-described experiments (see Fig. S4 in the supplemental material), and NBMPR (7 μM) failed to affect telaprevir antiviral activity (see Fig. S5 in the supplemental material).

These results clearly show that inhibition of ENT1-mediated ribavirin uptake significantly attenuates ribavirin antiviral effectiveness by reducing the accumulation level of the drug in the cells.

Effect of ENT1 mRNA knockdown on ribavirin anti-HCV activity. The above-mentioned results prompted us to investigate whether a small change in ENT1 activity would similarly affect ribavirin antiviral effectiveness. miRNA targeted to ENT1 mRNA was used in this examination. We found that when stably expressed in OR6 cells (OR6/miR-ENT1), miR-ENT1 reduced the ENT1 mRNA expression level to 72.5 ± 3.4% of that of the control cells (OR6/miR-Ng) without affecting the ENT2 mRNA expression level (Fig. 4A). Accordingly, the ribavirin uptake level in OR6/miR-ENT1 cells was about 66.7 ± 14.0% of that in OR6/miR-Ng cells (Fig. 4B). To determine the degree to which this ENT1 mRNA knockdown affected ribavirin antiviral action, concentration dependencies of ribavirin action in OR6/miR-ENT1 and OR6/miR-Ng cells were characterized. We found that the EC_{50} of ribavirin in OR6/miR-ENT1 cells was 212 ± 11 μM, which was significantly higher than the EC_{50} in OR6/miR-Ng cells (143 ± 33 μM; $P = 0.013$) (The results of the individual experiments are shown in Fig. S3 in the supplemental material.) These results showed that even a small reduction in the ENT1 mRNA expression level could decrease the ribavirin uptake level, thus causing a reduction in the antiviral efficacy of the drug.

Toxicological analyses. Concurrent with the above-described experiments, the cytotoxic effects of ribavirin and other reagents on OR6 cells were examined independently and/or simultaneously (see the supplemental methods in the supplemental material). As shown in Table S2 and Fig. S6 of the supplemental materials, the lactate dehydrogenase (LDH) release assay results showed that no severe cytotoxicity in OR6 cells occurred in any treatments (less than 10%). Microscopic observation also showed that the cells were viable upon treatment with ribavirin (3,162 μM) together with NBMPR (100 μM) for 48 h (see Fig. S2 in the supplemental material). We further performed the MTS assay, which can detect different types of toxicity, to confirm the results of the LDH assay. The results showed that even though marginal toxicity was observed at the highest ribavirin and NBMPR concentrations tested (at most 25%), most treatments did not display severe cytotoxicity for OR6 cells (less than 10%; see Table S2 in the supplemental material).

DISCUSSION

In this paper, we provide results supporting our hypothesis that ENT1 plays an essential role in the anti-HCV activity of ribavirin

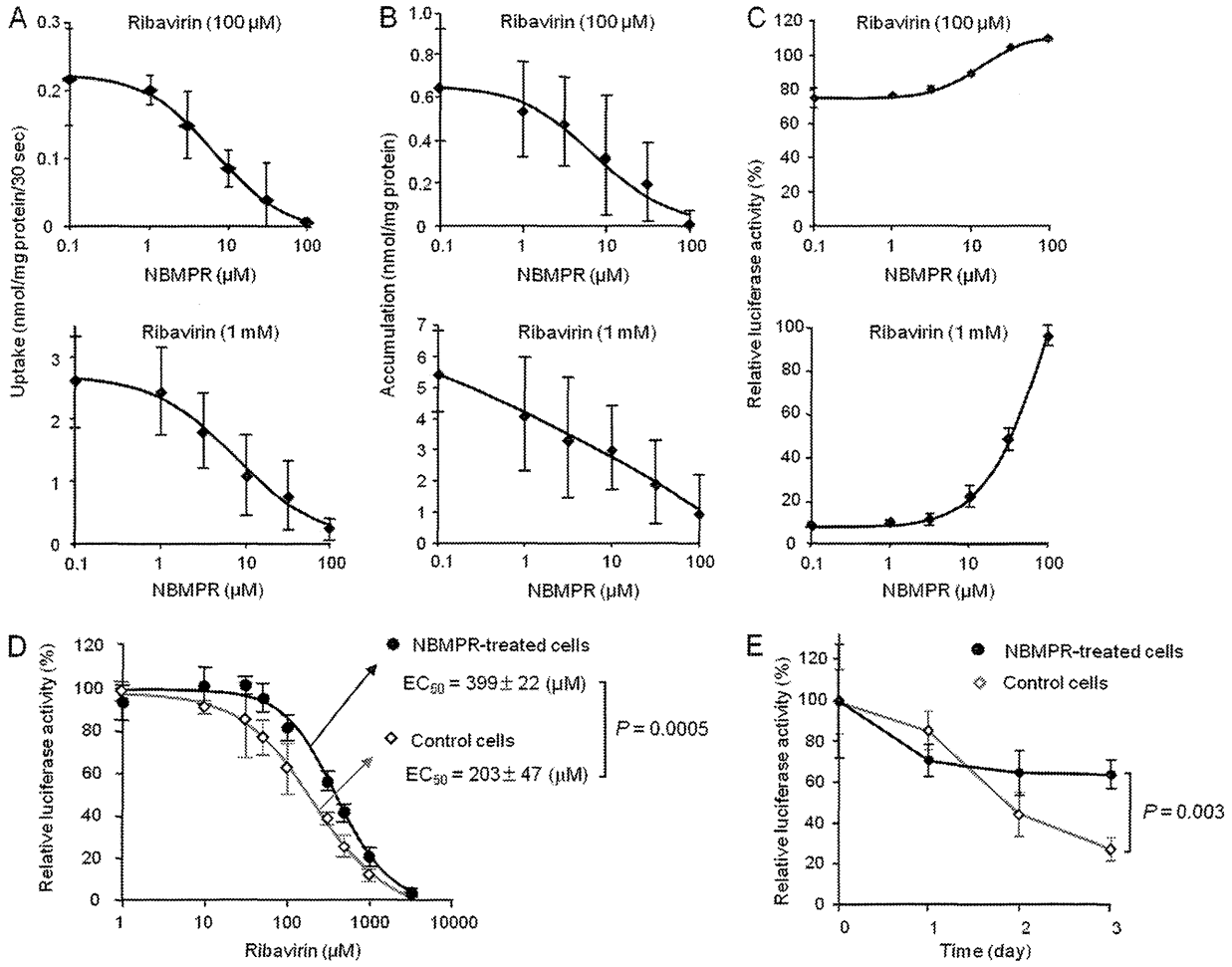

FIG 3 Inhibitory effect of NBMPR on ribavirin uptake, accumulation, and anti-HCV activity. The ribavirin concentration used in these experiments (A to C) was 100 μM or 1 mM, while the NBMPR concentrations used were 0.1, 1, 3, 10, 31, and 100 μM. (A) The effect of NBMPR on ribavirin uptake by OR6 cells was analyzed in Na^+-free KHB with NBMPR. Each value is the mean ± SD from five independent experiments, each performed in duplicate. (B) The effect of NBMPR on ribavirin accumulation in OR6 cells was analyzed by measuring the level of the drug within the cells, in the presence of NBMPR, for 48 h. Each value is the mean ± SD from three independent experiments, each performed in duplicate. (C) The effect of NBMPR on the anti-HCV activity of ribavirin in OR6 cells was analyzed by measuring the level of the luciferase activity, in the presence of NBMPR, for 48 h. The value of relative luciferase activity without ribavirin and NBMPR was set to 100%. Each value is the mean ± SD from three independent experiments, each performed in triplicate. (D) The concentration dependency of ribavirin antiviral action in the presence of NBMPR was examined. The ribavirin concentrations used are shown in the legend to Fig. 1A. The NBMPR concentration was set to 7 μM, which is near the EC_{50} of NBMPR calculated from the results in panel A. The value of relative luciferase activity in the absence of ribavirin was set to 100%. (E) The time dependency of ribavirin antiviral action in the presence of NBMPR was then examined. The ribavirin concentration was set to 150 μM, while the NBMPR concentration was still 7 μM. The value of relative luciferase activity in the absence of ribavirin at each time point was set to 100%.

through detailed characterization of the antiviral activity of the drug and its association with ENT1-mediated uptake in OR6 cells.

Our results showed that the concentration and time dependency of ribavirin antiviral activity was closely associated with its accumulation in OR6 cells. This association is supported by several reports. For example, it has been reported that larger ribavirin accumulations were associated with significant decreases in the intracellular GTP pool (13) or with higher antiviral potency against the Hantaan virus (14). Therefore, it is considered likely that continuous ribavirin accumulation in hepatic cells at the higher levels, which are achieved by the sustained and higher ribavirin extracellular concentrations, is critical to the antiviral efficacy of the drug.

Due to its hydrophilicity, ribavirin requires a "gate" to penetrate the plasma membrane of cells prior to its accumulation. Our results clearly show that ENT1 provides this gate, thus facilitating the drug's import into and accumulation in OR6 cells. Since we recently showed that ENT1 is also exclusively involved in ribavirin uptake in human hepatocytes, which has a ribavirin uptake profile similar to that of OR6 cells (6), it is considered likely that this ENT1 role can probably be extended to human hepatocytes as well. The mode of ENT1-mediated ribavirin uptake in OR6 cells, as well as human hepatocytes, was represented by a linear increase in the uptake level along with an increase in extracellular ribavirin concentration (6; also this study). This uptake feature was the most probable reason why the higher extracellular ribavirin concentration resulted in a stronger antiviral effect in OR6 cells but might also explain why clinical findings show that a higher exposure to ribavirin leads to the better virologic response in HCV genotype-1 patients (11, 17). Therefore, our results, together with

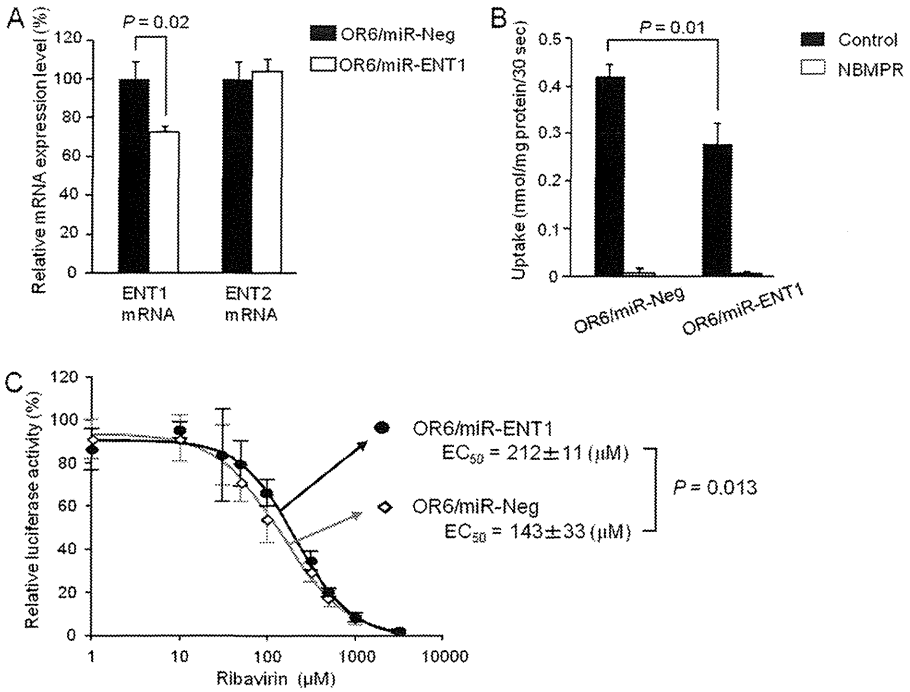

FIG 4 Effect of ENT1 mRNA knockdown on anti-HCV activity of ribavirin. (A) The expression levels of ENT1 and ENT2 mRNA were determined by real-time PCR. Abundance is shown relative to the level of ENT1 or ENT2 mRNA in OR6/miR-Ng cells. Each value is the mean plus SD from three independent experiments, each performed in duplicate. (B) Ribavirin (100 μM) uptake by OR6/miR-ENT1 and OR6/miR-Ng cells was analyzed in Na^+-free KHB in the absence (control) or presence of 100 μM NBMPR. Each value is the mean plus SD of transport activity from three independent experiments, each performed in duplicate. (C) The concentration dependency of ribavirin in OR6/miR-Ng and OR6/miR-ENT1 cells was then examined. The ribavirin concentrations used are shown in the legend to Fig. 1A. The relative luciferase activity value in the absence of ribavirin in each cell line was set to 100%. Each value is the mean ± SD of relative luciferase activity from four independent experiments, each performed in triplicate.

the other findings, indicate that ENT1 plays an indispensable role in ribavirin antiviral activity.

The importance of ENT1 in ribavirin antiviral activity was further underscored by the results of both the ENT1 knockdown and uptake inhibition experiments using NBMPR. It is noteworthy that even a small reduction of ENT1 activity significantly weakened ribavirin's antiviral potency. These results indicate that increasing or decreasing ENT1 activity level in the cells results in stronger or weaker ribavirin efficacy by increasing or reducing the uptake of the drug, even if extracellular ribavirin concentrations and exposure durations are constant. Therefore, it can be concluded that the ENT1-mediated ribavirin uptake level determines the level of ribavirin antiviral activity in OR6 cells and, presumably, in human hepatocytes.

The above-mentioned findings and suppositions prompt us to propose the following two possibilities (see Fig. S7 in the supplemental material). One is that patients with higher ENT1 activity levels in hepatocytes could more likely attain RVR (defined as a faster and stronger ribavirin antiviral effect in the early stage of the treatment) than those with lower ENT1 activity levels, when other factors affecting the treatment outcome are similar. The mechanisms underlying the interindividual difference in the hepatic ENT1 activity level remain unclear, but SNPs are promising candidates for the causal factors that result in the difference. Since two intronic SNPs have been revealed to be associated with RVR (and SVR) (12, 18), investigations should be conducted to determine whether these SNPs have a positive effect on the hepatic ENT1 expression level.

The other possibility is that the hepatic uptake of ribavirin by ENT1 could be hindered by coadministered chemicals, thus resulting in attenuation of the treatment response in some patients, as shown in Fig. 3. Although there have been no clinical reports supporting this possibility, preceding studies have been performed to determine whether hepatic uptake inhibition of pravastatin and metformin, which are hepatocyte-targeting drugs, reduces their effectiveness (1). These drugs are known substrates for hepatic organic ion transporters, and it has been shown that aberrations in these transporters significantly impair their *in vivo* functions (2, 15). Since, due to attendant complications or other chronic diseases, several drugs are often coprescribed along with ribavirin during treatment regimens, it may be worth considering whether interactions between ribavirin and other drugs at the point of ENT1-mediated uptake can affect the treatment response.

Exploration of these possibilities must await further studies aimed at clarification of the factors affecting the hepatic ENT1 activity level, including the above-described SNP studies and ribavirin-drug interaction studies. The results obtained from such studies could contribute not only to a better understanding of the mode of action of ENT1 on ribavirin antiviral activity but also to identification of the associated markers for RVR or null responses in clinical settings.

It should be noted that, unexpectedly, ENT1 activity was found to be insensitive to inhibition by NBMPR in the nanomolar range in OR6 cells. This was not due to nucleotide alterations in ENT1 cDNA of OR6 cells (Iikura, unpublished). Since OR6 cells were

derived from Huh-7 cells, we examined the sensitivity of ENT1 to inhibition of NBMPR using Huh-7 cells and obtained results similar to those obtained with OR6 cells (Iikura, unpublished). Therefore, the lower sensitivity of ENT1 to NBMPR in OR6 cells was thought to have originated from the Huh-7 cells. Although the reason for the altered sensitivity of ENT1 to NBMPR remains unknown at this time, it is believed that the cell-specific posttranslational modification might be involved. It has been reported that defective glycosylation of ENT1 leads to decreased affinity for NBMPR (19). Therefore, it can be speculated that the type or structure of glycochain and/or other modifications could be responsible for decreased affinity of ENT1 of OR6/Huh-7 cells for NBMPR. Further studies aimed at ascertaining the reason might provide novel insights into the biology of ENT1.

Finally, we briefly discuss the static cytotoxic effects of ribavirin and NBMPR on OR6 cells. According to the results of toxicological analyses, these reagents (at most concentrations tested) did not cause severe toxicity in OR6 cells (less than 10%), and only marginal toxicity was found in treatment of the reagents at the highest concentrations tested in an MTS assay. In contrast, blasticidin S treatment (20 ng/ml) significantly damaged the cells (>50% in the MTS assay [Iikura, unpublished]). Therefore, it is assumed that OR6 cells possess inherent resistance to ribavirin and NBMPR, and this factor might be related to the relatively high EC_{50} of ribavirin. Although we do not know the reason for the behavior of the cells, it is unlikely that the limited toxicity would give rise to a question regarding the present results. In actuality, 100 μM NBMPR treatment, which caused marginal toxicity, did not affect HCV replication activity (see Fig. S4 in the supplemental material).

In conclusion, we have clearly demonstrated that ENT1 plays an indispensable role in ribavirin antiviral activity by facilitating the uptake and accumulation of the drug in OR6 cells, thereby indicating that ENT1 provides a gate that is essential to the success of ribavirin's mission. Our study limitations include an *in vitro* HCV model system using hepatoma cells and no *in vivo* evidence of association between hepatic ENT1 activity and ribavirin efficacy. Nevertheless, our results, together with the literature, strongly suggest that ENT1 also plays the determinant role in the antiviral efficacy of ribavirin in the human liver during the course of anti-HCV therapy. Accordingly, it is believed that our results, as well as the ideas described in this paper, will encourage further studies aimed at the clarification of the clinical importance of ENT1 in anti-HCV therapy.

ACKNOWLEDGMENTS

This work was supported by a grant (20790128) from the Ministry of Education, Sciences, Sports and Culture of Japan and partially supported by a Special Funds for Education and Research (Development of SPECT Probes for Pharmaceutical Innovation) from the Ministry of Education, Culture, Sports, Science and Technology, Japan, and a research grant from the Nakatomi Foundation (Tokyo, Japan).

REFERENCES

1. **Bachmakov I, Glaeser H, Fromm MF, König J.** 2008. Interaction of oral antidiabetic drugs with hepatic uptake transporters: Focus on organic anion transporting polypeptides and organic cation transporter 1. Diabetes 57:1463–1469.
2. **Becker ML, et al.** 2009. Genetic variation in the organic cation transporter 1 is associated with metformin response in patients with diabetes mellitus. Pharmacogenomics J. 9:242–247.
3. **Burke T, Lee S, Ferguson PJ, Hammond JR.** 1998. Interaction of 2′,2′-difluorodeoxycytidine (gemcitabine) and formycin B with the Na^+-dependent and -independent nucleoside transporters of Ehrlich ascites tumor cells. J. Pharmacol. Exp. Ther. **286**:1333–1340.
4. **Dixit NM, Perelson AS.** 2006. The metabolism, pharmacokinetics and mechanisms of antiviral activity of ribavirin against hepatitis C virus. Cell. Mol. Life Sci. **63**:832–842.
5. **Fried MW, et al.** 2002. Peginterferon alfa-2a plus ribavirin for chronic hepatitis C virus infection. N. Engl. J. Med. **347**:975–982.
6. **Fukuchi Y, Furihata T, Hashizume M, Iikura M, Chiba K.** 2010. Characterization of ribavirin uptake systems in human hepatocytes. J. Hepatol. **52**:486–492.
7. **Hofmann WP, Herrmann E, Sarrazin C, Zeuzem S.** 2008. Ribavirin mode of action in chronic hepatitis C: from clinical use back to molecular mechanisms. Liver Int. **28**:1332–1343.
8. **Ikeda M, et al.** 2005. Efficient replication of a full-length hepatitis C virus genome, strain O, in cell culture, and development of a luciferase reporter system. Biochem. Biophys. Res. Commun. **329**:1350–1359.
9. **Kong W, Engel K, Wang J.** 2004. Mammalian nucleoside transporters. Curr. Drug Metab. **5**:63–84.
10. **Leung GP, Man RY, Tse CM.** 2005. Effect of thiazolidinediones on equilibrative nucleoside transporter-1 in human aortic smooth muscle cells. Biochem. Pharmacol. **70**:355–362.
11. **Lindahl K, Stahle L, Bruchfeld A, Schvarcz R.** 2005. High-dose ribavirin in combination with standard dose peginterferon for treatment of patients with chronic hepatitis C. Hepatology **41**:275–279.
12. **Morello J, et al.** 2010. Influence of a single nucleotide polymorphism at the main ribavirin transporter gene on the rapid virological response to pegylated interferon-ribavirin therapy in patients with chronic hepatitis C virus infection. J. Infect. Dis. **202**:1185–1191.
13. **Smee DF, Matthews TR.** 1986. Metabolism of ribavirin in respiratory syncytial virus-infected and uninfected cells. Antimicrob. Agents Chemother. **30**:117–121.
14. **Sun Y, Chung DH, Chu YK, Jonsson CB, Parker WB.** 2007. Activity of ribavirin against Hantaan virus correlates with production of ribavirin-5′-triphosphate, not with inhibition of IMP dehydrogenase. Antimicrob. Agents Chemother. **51**:84–88.
15. **Tachibana-Iimori R, et al.** 2004. Effect of genetic polymorphism of OATP-C (SLCO1B1) on lipid-lowering response to HMG-CoA reductase inhibitors. Drug Metab. Pharmacokinet. **19**:375–380.
16. **Thomas E, et al.** 2011. Ribavirin potentiates interferon action by augmenting interferon-stimulated gene induction in hepatitis C virus cell culture models. Hepatology **53**:32–41.
17. **Tsubota A, Hirose Y, Izumi N, Kumada H.** 2003. Pharmacokinetics of ribavirin in combined interferon-alpha 2b and ribavirin therapy for chronic hepatitis C virus infection. Br. J. Clin. Pharmacol. **55**:360–367.
18. **Tsubota A, et al.** 2011. Contribution of ribavirin transporter gene polymorphism to treatment response in peginterferon plus ribavirin therapy for HCV genotype 1b patients. Liver Int. [Epub ahead of print.10.1111/j.1478–3231.2011.02727.x.
19. **Vickers MF, et al.** 1999. Functional production and reconstitution of the human equilibrative nucleoside transporter (hENT1) in Saccharomyces cerevisiae. Interaction of inhibitors of nucleoside transport with recombinant hENT1 and a glycosylation-defective derivative (hENT1/N48Q). Biochem. J. **339**:21–32.
20. **Ward JL, Sherali A, Mo ZP, Tse CM.** 2000. Kinetic and pharmacological properties of cloned human equilibrative nucleoside transporters, ENT1 and ENT2, stably expressed in nucleoside transporter-deficient PK15 cells. J. Biol. Chem. **275**:8375–8381.
21. **Yamamoto T, et al.** 2007. Ribavirin uptake by cultured human choriocarcinoma (BeWo) cells and Xenopus laevis oocytes expressing recombinant plasma membrane human nucleoside transporters. Eur. J. Pharmacol. **557**:1–8.
22. **Yao SY, et al.** 2002. Functional and molecular characterization of nucleobase transport by recombinant human and rat equilibrative nucleoside transporters 1 and 2. J. Biol. Chem. **277**:24938–24948.

PLOS ONE

Inhibition of Both Protease and Helicase Activities of Hepatitis C Virus NS3 by an Ethyl Acetate Extract of Marine Sponge *Amphimedon* sp.

Yuusuke Fujimoto[1], Kazi Abdus Salam[2☯], Atsushi Furuta[3,4☯], Yasuyoshi Matsuda[3,4], Osamu Fujita[3,4], Hidenori Tani[5], Masanori Ikeda[6], Nobuyuki Kato[6], Naoya Sakamoto[7], Shinya Maekawa[8], Nobuyuki Enomoto[8], Nicole J. de Voogd[9], Masamichi Nakakoshi[10], Masayoshi Tsubuki[10], Yuji Sekiguchi[3], Satoshi Tsuneda[4], Nobuyoshi Akimitsu[2], Naohiro Noda[3,4], Atsuya Yamashita[1]*, Junichi Tanaka[11]*, Kohji Moriishi[1]*

1 Department of Microbiology, Division of Medicine, Graduate School of Medicine and Engineering, University of Yamanashi, Yamanashi, Japan, **2** Radioisotope Center, The University of Tokyo, Tokyo, Japan, **3** Biomedical Research Institute, National Institute of Advanced Industrial Science and Technology, Ibaraki, Japan, **4** Department of Life Science and Medical Bioscience, Waseda University, Tokyo, Japan, **5** Research Institute for Environmental Management Technology, National Institute of Advanced Industrial Science and Technology, Ibaraki, Japan, **6** Department of Tumor Virology, Okayama University Graduate School of Medicine, Dentistry, and Pharmaceutical Sciences, Okayama, Japan, **7** Department of Gastroenterology and Hepatology, Hokkaido University Graduate School of Medicine, Sapporo, Japan, **8** First Department of Internal Medicine, Faculty of Medicine, University of Yamanashi, Yamanashi, Japan, **9** Netherlands Centre for Biodiversity Naturalis, Leiden, The Netherlands, **10** Institute of Medical Chemistry, Hoshi University, Tokyo, Japan, **11** Department of Chemistry, Biology and Marine Science, University of the Ryukyus, Okinawa, Japan

Abstract

Combination therapy with ribavirin, interferon, and viral protease inhibitors could be expected to elicit a high level of sustained virologic response in patients infected with hepatitis C virus (HCV). However, several severe side effects of this combination therapy have been encountered in clinical trials. In order to develop more effective and safer anti-HCV compounds, we employed the replicon systems derived from several strains of HCV to screen 84 extracts from 54 organisms that were gathered from the sea surrounding Okinawa Prefecture, Japan. The ethyl acetate-soluble extract that was prepared from marine sponge *Amphimedon* sp. showed the highest inhibitory effect on viral replication, with EC_{50} values of 1.5 and 24.9 μg/ml in sub-genomic replicon cell lines derived from genotypes 1b and 2a, respectively. But the extract had no effect on interferon-inducing signaling or cytotoxicity. Treatment with the extract inhibited virus production by 30% relative to the control in the JFH1-Huh7 cell culture system. The *in vitro* enzymological assays revealed that treatment with the extract suppressed both helicase and protease activities of NS3 with IC_{50} values of 18.9 and 10.9 μg/ml, respectively. Treatment with the extract of *Amphimedon* sp. inhibited RNA-binding ability but not ATPase activity. These results suggest that the novel compound(s) included in *Amphimedon* sp. can target the protease and helicase activities of HCV NS3.

Citation: Fujimoto Y, Salam KA, Furuta A, Matsuda Y, Fujita O, et al. (2012) Inhibition of Both Protease and Helicase Activities of Hepatitis C Virus NS3 by an Ethyl Acetate Extract of Marine Sponge *Amphimedon* sp.. PLoS ONE 7(11): e48685. doi:10.1371/journal.pone.0048685

Editor: Tetsuo Takehara, Osaka University Graduate School of Medicine, Japan

Received June 16, 2012; **Accepted** October 1, 2012; **Published** November 7, 2012

Funding: This work was supported in part by grants-in-aid from the Ministry of Health, Labor, and Welfare (http://www.mhlw.go.jp/) and from the Ministry of Education, Culture, Sports, Science, and Technology of Japan (http://www.mext.go.jp/). The funders had no role in study design, data collection and analysis, decision to publish, or preparation of the manuscript.

Competing Interests: The authors have declared that no competing interests exist.

* E-mail: atsuyay@yamanashi.ac.jp (AY); jtanaka@sci.u-ryukyu.ac.jp (JT); kmoriishi@yamanashi.ac.jp (KM)

☯ These authors contributed equally to this work.

Introduction

Hepatitis C virus (HCV) is an enveloped RNA virus of the genus *Hepacivirus* of the *Flaviviridae* family. More than 170 million patients persistently infected with HCV have been reported worldwide, leading to liver diseases including steatosis, cirrhosis, and hepatocellular carcinoma [1,2]. The genome of HCV is characterized as a single positive-strand RNA with a nucleotide length of 9.6 kb, flanked by 5′ and 3′-untranslated regions (UTRs). The genomic RNA encodes a large polyprotein consisting of approximately 3,000 amino acids [3], which is translated under the control of an internal ribosome entry site (IRES) located within the 5′-UTR of the genomic RNA [4]. The translated polyprotein is cleaved by host and viral proteases, resulting in 10 mature viral proteins [3]. The structural proteins, consisting of core, E1, and E2, are located in the N-terminal quarter of the polyprotein, followed by viroporin p7, which has not yet been classified into a structural or nonstructural protein. Further cleavage of the remaining portion by viral proteases produces six nonstructural proteins–NS2, NS3, NS4A, NS4B, NS5A, and NS5B–which form a viral replication complex with various host factors. The viral protease NS2 cleaves its own C-terminal between NS2 and NS3. After that, NS3 cleaves the C-terminal ends of NS3 and NS4A and then forms a complex with NS4A. The NS3/4A complex becomes a fully active form to cleave the C-terminal parts of the polyprotein, including nonstructural proteins. NS3 also possesses

RNA helicase activity to unwind the double-stranded RNA during the synthesis of genomic RNA [5,6].

Although the previous standard therapy, combining pegylated interferon with ribavirin, was effective in only about half of patients infected with genotype 1, the most common genotype worldwide [7–9], recent biotechnological advances have led to the development of a novel therapy using anti-HCV agents that directly target HCV proteins or host factors required for HCV replication and have improved the sustained virologic response (SVR) [10–12]. Telaprevir and boceprevir, which are categorized as advanced NS3/4A protease inhibitors, were recently approved for the treatment of chronic hepatitis C patients infected with genotype 1 [13,14]. The triple combination therapy with pegylated interferon, ribavirin, and telaprevir improved SVR by 77% in patients infected with genotype 1 [15]. However, this therapy exhibits side effects including rash, severe cutaneous eruption, influenza-like symptoms, cytopenias, depression, and anemia [7,16,17]. Furthermore, the possibility of the emergence of drug-resistant viruses is a serious problem with therapies that use antiviral compounds [18,19].

Recent technical advances in the determination of molecular structures and the synthesis of chemical compounds have led to the development of various drugs based on natural products, especially drugs identified from terrestrial plants and microbes [20–22]. Marine organisms, including plants and animals, were recently established as representative of a natural resource library for drug development. Potent biological activity is often found in products isolated from marine organisms because of their novel molecular structures [23,24]. Trabectedin (Yondelis), cytarabine (Ara-C), and eribulin (Halaven), which are known as antitumor drugs, were developed from compounds found in marine organisms [25].

In this study, we screened 84 extracts prepared from 54 marine organisms by using replicon cell lines derived from HCV genotype 1b and attempted to identify the extract that inhibits HCV RNA replication. A marine organism may produce anti-HCV agent(s) that could inhibit the protease and helicase activities of NS3.

Results

Effect of the Extract from Marine Sponge and Tunicate on HCV Replication

We prepared methanol (MeOH)- and ethyl acetate (EtOAc)-soluble extracts from 54 marine organisms in order to test which of these extracts could best suppress HCV replication. Each extract was added at 25 μg/ml to the culture supernatant of HCV replicon cell lines derived from O and Con1 strains of genotype 1b, which produce the luciferase/neomycin hybrid protein depending on RNA replication. Luciferase activity and cell viability were measured 72 h after treatment with the extracts (Table 1). The extracts exhibiting more than 85% cell viability and lower than 15% luciferase activity were selected as arbitrary candidates for the extract including anti-HCV compounds. The EtOAc-extract prepared from sample C-29 (C-29EA) was selected as a candidate in both cell lines. Thus, the anti-HCV activity of extract C-29EA was tested.

The EtOAc-soluble extract C-29EA was prepared from the marine sponge *Amphimedon* sp. (Fig. 1A), which inhabits the sea surrounding Okinawa Prefecture, Japan. HCV replication was inhibited in a dose-dependent manner but did not exhibit cytotoxicity when replicon cells were treated with C-29EA (Fig. 1 B). The extract C-29EA exhibited EC_{50} values of 1.5 μg/ml (Table 2). Furthermore, treatment with C-29EA suppressed the HCV replication derived from the genotype 2a strain JFH1 with an EC_{50} of 24.9 μg/ml, irrespective of cell viability (Fig. 2A and Table 2). Extract C-29EA also inhibited the production of infectious viral particles, viral RNA, and core protein from JFH1-infected cells in the supernatant (Fig. 2B and C). These results suggest that the marine sponge *Amphimedon* sp. possesses anti-HCV agents.

Effect of Extract C-29EA on IRES-dependent Translation

Extract C-29EA had the most potent inhibitory activity against HCV replication. The viral replication (Fig. 1 B and 2 A) and viral proteins (Fig. 3 A and B) in replicon cell lines derived from genotype 1b strain Con1 and 2a strain JFH1 were decreased 72 h after treatment in a dose-dependent manner. HCV protein has been translated based on the positive-sense viral RNA in an IRES-dependent manner. The replicon RNA of HCV is composed of the 5′-UTR of HCV, indicator genes (a luciferase-fused drug-resistant gene), encephalomyocarditis virus (EMCV) IRES, the viral genes encoding complete or nonstructural proteins, and the 3′-UTR of HCV, in that order [26]. The replicon RNA replicated autonomously in several HCV replication-permissive cell lines derived from several hepatoma cell lines. Nonstructural proteins in replicon cells were polycistronically translated through EMCV IRES. The cap-dependent translated mRNA, including *Renilla* luciferase, EMCV IRES, and the firefly luciferase/neomycin-resistant gene, in that order, was constructed to examine the effect of the extract on EMCV-IRES-dependent translation (Fig. 3C). When the mRNA expression was transcribed by an EF promoter of the transfected plasmid in the presence of C-29EA, the ratio of firefly luciferase activity to *Renilla* luciferase activity was not changed (Fig. 3C). This suggested that treatment with C-29EA exhibited no effect on EMCV-IRES-dependent translation. Furthermore, treatment with C-29EA did not significantly affect the activity of HCV IRES that was used instead of EMCV IRES in the system described above (Fig. 3D). Thus, these results suggest that treatment with C-29EA exhibits no effect on EMCV- or HCV-IRES-dependent translation.

Effect of C-29EA on the Interferon Signaling Pathway

It has been well known that HCV replication in cultured cells is potently inhibited by interferon [27,28]. We examined whether or not treatment with C-29EA elicits an interferon-inducible gene from replicon cells. The replicon cells were treated with various concentrations of interferon-alpha 2b or 15 μg of C-29EA per milliliter. The treated cells were harvested at 72 h post-treatment. The interferon-inducible gene 2′, 5′-OAS, was induced with IFN-alpha 2b but not with a 10-times EC_{50} concentration of C-29EA (Fig. 4). These results suggest that the inhibitory effect of C-29EA on the replication of the HCV replicon is independent of the IFN signaling pathway.

Effect of C-29EA on the NS3 Helicase Activity

We previously established an assay system for unwinding HCV activity based on photoinduced electron transfer (PET) [29,30]. The fluorescent dye (BODIPY FL) is attached to the cytosine at the 5′-end of the fluorescent strand and quenched by the guanine base at the 3′-end of the complementary strand via PET. When helicase unwinds the double-strand RNA substrate, the fluorescence of the dye emits a bright light upon the release of the dye from the guanine base. The capture strand, which is complementary to the complementary strand, prevents the reannealing of the unwound duplex. Treatment with C-29EA inhibited the helicase activity in a dose-dependent manner, with an IC_{50} value of 18.9 μg/ml (Fig. 5A). We confirmed the effect of C-29EA on NS3 helicase unwinding activity by the RNA helicase assay using ^{32}P-labeled double-stranded RNA (dsRNA) as a substrate. Treatment

Table 1. Effect of marine organism extracts on HCV replication and cell viability.

No.	Sample	Luciferase activity (% of control)		Cell viability (% of control)		Phylum	Specimen	Extract	Site
		O	Con1	O	Con1				
1	A-1	10	111	105	104	Sponge	*Unidentified*	MeOH	A
2	A-2	82	209	91	132	Soft coral	*Briareum*	MeOH	A
3	A-3	87	177	54	110	Tunicate	*unidentified*	MeOH	A
4	A-4	82	186	84	100	Sponge	*Liosina*	MeOH	A
5	B-5	110	165	86	110	Sponge	*unidentified*	MeOH	B
6	B-6	70	149	103	119	Sponge	*Xestospongia*	MeOH	B
7	B-7	89	191	111	144	Sponge	*Epipolasis*	MeOH	B
8	B-8	89	182	115	132	Sponge	*unidentified*	MeOH	B
9	B-9	57	72	92	124	Sponge	*Strongylophora*	MeOH	B
10	B-10	106	182	73	96	Sponge	*Stylotella aurantium*	MeOH	B
11	C-12	96	162	114	98	Sponge	*Epipolasis*	MeOH	B
12	C-13	123	141	91	103	Sponge	*unidentified*	MeOH	B
13	C-14	89	175	77	100	Sponge	*Hippospongia*	MeOH	B
14	C-16	80	177	108	88	Sponge	*unidentified*	MeOH	B
15	C-18	119	170	93	94	Sponge	*unidentified*	MeOH	B
16	C-19	0	0	0	4	Sponge	*unidentified*	MeOH	B
17	C-20	101	158	61	106	Sponge	*Xestospongia testudinaria*	MeOH	B
18	C-21	85	161	83	102	Sponge	*unidentified*	MeOH	B
19	C-22	109	88	38	89	Sponge	*unidentified*	MeOH	B
20	C-23	94	156	32	90	Sponge	*unidentified*	MeOH	B
21	C-24	118	86	42	94	Sponge	*Theonella*	MeOH	B
22	C-25	82	111	91	106	Sponge	*unidentified*	MeOH	B
23	C-27	0	0	15	2	Sponge	*unidentified*	MeOH	B
24	C-28	90	166	30	90	Sponge	*Petrosia*	MeOH	B
25	C-29	65	151	29	101	Sponge	*Amphimedon*	MeOH	B
26	D-31	81	127	55	91	Tunicate	*unidentified*	MeOH	C
27	D-32	80	141	47	93	Sponge	*unidentified*	MeOH	C
28	D-33	88	153	72	90	Gorgonian	*Junceella fragilis*	MeOH	C
29	E-35	114	156	40	118	Sponge	*Phyllospongia sp.*	MeOH	C
30	E-36	80	125	69	116	Tunicate	*Didemnum molle*	MeOH	C
31	E-37	88	129	54	108	Sponge	*Xestospongia sp.*	MeOH	C
32	E-38	70	153	35	112	Sponge	*unidentified*	MeOH	C
33	F-40	119	170	38	104	Sponge	*unidentified*	MeOH	C
34	F-41	88	166	48	101	Soft coral	*unidentified*	MeOH	C
35	G-42	113	157	31	126	Sponge	*unidentified*	MeOH	D
36	H-43	83	0	39	5	Sponge	*unidentified*	MeOH	D
37	J-44	62	183	27	105	Sponge	*Cinachyra*	MeOH	D
38	J-45	96	140	47	103	Sponge	*Liosina*	MeOH	D
39	J-46	83	149	77	102	Sponge	*unidentified*	MeOH	D
40	J-47	94	37	40	111	Sponge	*unidentified*	MeOH	D
41	J-48	24	16	53	70	Sponge	*Stylotella*	MeOH	D
42	J-49	78	123	55	105	Sponge	*unidentified*	MeOH	D
43	J-50	93	138	51	108	Sponge	*unidentified*	MeOH	D
44	J-51	103	73	41	115	Sponge	*unidentified*	MeOH	D
45	J-52	162	237	113	131	Sponge	*unidentified*	MeOH	D
46	J-53	51	90	93	122	Tunicate	*Didemnum*	MeOH	D
47	J-54	42	90	113	124	Sponge	*unidentified*	MeOH	D

Table 1. Cont.

No.	Sample	Luciferase activity (% of control)		Cell viability (% of control)		Phylum	Specimen	Extract	Site
		O	Con1	O	Con1				
48	J-55	88	133	131	110	Jellyfish	*unidentified*	MeOH	D
49	J-56	28	51	113	103	Sponge	*unidentified*	MeOH	D
50	J-57	8	63	94	85	Tunicate	*Pseudodistoma kanoko*	MeOH	D
51	J-58	0	2	48	65	Sponge	*unidentified*	MeOH	D
52	J-59	0	2	45	71	Sponge	*unidentified*	MeOH	D
53	J-60	98	134	122	95	Annelid	*unidentified*	MeOH	D
54	A-2	0	1	6	15	Soft coral	*Briareum*	EtOAc	A
55	A-3	0	0	6	9	Tunicate	*unidentified*	EtOAc	A
56	A-4	22	36	74	76	Sponge	*Liosina*	EtOAc	A
57	B-5	33	107	69	93	Sponge	*unidentified*	EtOAc	B
58	B-6	0	0	5	8	Sponge	*Xestospongia*	EtOAc	B
59	B-7	0	0	5	9	Sponge	*Epipolasis*	EtOAc	B
60	B-8	0	0	2	46	Sponge	*unidentified*	EtOAc	B
61	B-9	0	0	8	14	Sponge	*Strongylophora*	EtOAc	B
62	B-10	0	0	3	8	Sponge	*Stylotella aurantium*	EtOAc	B
63	C-12	0	0	4	14	Sponge	*Epipolasis*	EtOAc	B
64	C-13	0	0	4	5	Sponge	*unidentified*	EtOAc	B
65	C-14	48	119	82	102	Sponge	*Hippospongia*	EtOAc	B
66	C-15	0	0	8	11	Sponge	*unidentified*	EtOAc	B
67	C-18	0	0	4	3	Sponge	*unidentified*	EtOAc	B
68	C-19	23	76	63	109	Sponge	*unidentified*	EtOAc	B
69	C-20	34	32	63	112	Sponge	*Xestospongia testudinaria*	EtOAc	B
70	C-21	1	0	52	12	Sponge	*unidentified*	EtOAc	B
71	C-22	76	34	74	110	Sponge	*unidentified*	EtOAc	B
72	C-24	0	0	20	7	Sponge	*Theonella*	EtOAc	B
73	C-26	41	43	80	110	Sponge	*unidentified*	EtOAc	B
74	C-27	1	0	35	40	Sponge	*unidentified*	EtOAc	B
75	C-28	68	62	82	115	Sponge	*Petrosia*	EtOAc	B
76	C-29	10	11	93	88	Sponge	*Amphimedon*	EtOAc	B
77	D-31	20	71	85	120	Tunicate	*Eudistoma*	EtOAc	C
78	D-33	0	0	5	7	Gorgonian	*Junceella fragilis*	EtOAc	C
79	E-35	0	0	4	5	Sponge	*Phyllospongia sp.*	EtOAc	C
80	E-36	71	83	75	100	Tunicate	*Didemnum molle*	EtOAc	C
81	F-40	72	110	87	130	Sponge	*unidentified*	EtOAc	C
82	F-41	8	33	73	104	Soft coral	*unidentified*	EtOAc	C
83	H-43	0	197	4	119	Sponge	*unidentified*	EtOAc	D
84	J-46	113	58	103	126	Sponge	*unidentified*	EtOAc	D

There are a total of 54 marine organisms, while 84 extracts were prepared from them with ethyl acetate and/or methanol. Aragusuku, Iriomote, Kohama, and Ishigaki islands are indicated by A, B, C, and D, respectively, in the collection-site column?(right end). EtOAc: Ethyl acetate; MeOH: Methanol.
doi:10.1371/journal.pone.0048685.t001

with C-29EA inhibited dsRNA dissociation at a concentration of 16 μg/ml and above (Fig. 5B).

The unwinding ability of HCV helicase depends on ATP binding, ATP hydrolysis, and RNA binding [30,31]. We examined the effect of C-29EA on the ATPase activity of NS3. The ratio of free phosphate (^{32}P-Pi) to ATP (^{32}P-ATP) was determined in the presence of C-29EA. The reaction was carried out between 16 and 250 μg of C-29EA per milliliter. The ATPase activity of NS3 helicase was not inhibited (Fig. 6A), although the helicase activity was decreased to less than 20% in the presence of 50 μg of C-29EA per milliliter (Fig. 5A). Next, we examined the effect of C-29EA on the binding of NS3 helicase to single-strand RNA (ssRNA). A gel-mobility shift assay was employed to estimate the binding activity of NS3 to the 21-mer of ssRNA. The binding of NS3 to ssRNA was inhibited by C-29EA in a dose-dependent manner (Fig. 6 B and C). These results suggest that treatment with C-29EA inhibits the helicase activity of NS3 by suppressing RNA binding.

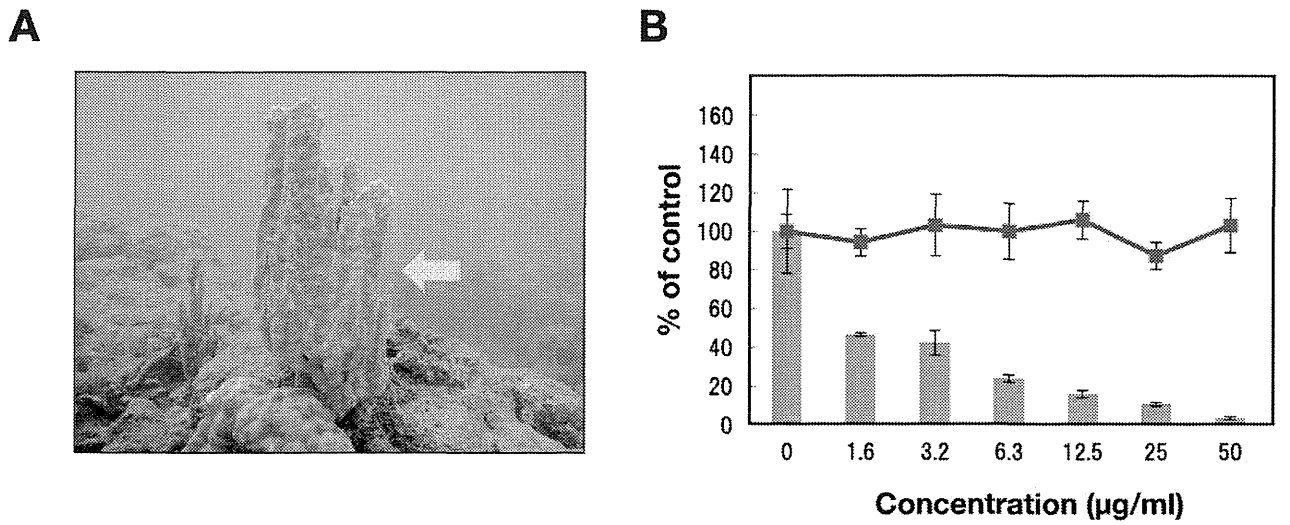

Figure 1. Effect of the extract prepared from a marine sponge on viral replication in the replicon cell line derived from viral genotype 1b. (A) *Amphimedon* sp. belongs to a marine sponge. The ethyl acetate fraction prepared from the marine organism was designated C-29EA in this study. (B) The Huh7 cell line, including the subgenomic replicon RNA of genotype 1b strain Con1, was incubated in medium containing various concentrations of C-29EA or DMSO (0). Luciferase and cytotoxicity assays were carried out as described in Materials and Methods. Error bars indicate standard deviation. The data represent three independent experiments.
doi:10.1371/journal.pone.0048685.g001

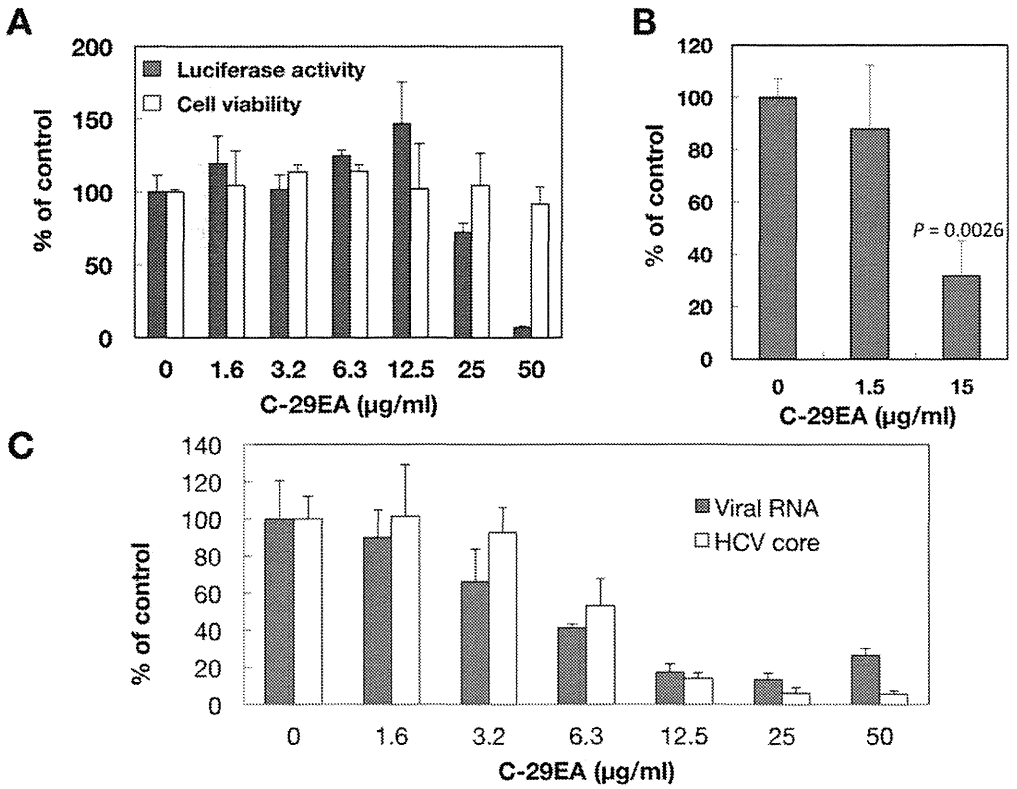

Figure 2. Effect of C-29EA extract on viral replication in the replicon cell line derived from viral genotype 2a. (A) The Huh7 cell line, including the subgenomic replicon RNA of genotype 2a strain JFH1, was incubated in medium containing various concentrations of C-29EA or DMSO (0). Luciferase and cytotoxicity assays were carried out as described in Materials and Methods. (B) The Huh7 OK1 cell line infected with HCVcc JFH1 was incubated with various concentrations of C-29EA or DMSO (0). The virus titers were determined by a focus-forming assay. The significance of differences in the means was determined by Student's *t*-test. (C) Amounts of viral RNA and core protein were estimated by qRT-PCR and ELISA, respectively. Error bars indicate standard deviation. The data represent three independent experiments. Treatment with DMSO corresponds to '0'.
doi:10.1371/journal.pone.0048685.g002

Table 2. Effect of C29EA on HCV replication.

HCV strain (genotype)	EC_{50} (μg/ml)[a]	CC_{50} (μg/ml)[b]	SI[c]
Con 1 (1b)	1.5	>50	>33.3
JFH1 (2a)	24.9	>50	>2.3

[a]: Fifty percent effective concentration based on the inhibition of HCV replication.
[b]: Fifty percent cytotoxicity concentration based on the reduction of cell viability.
[c]: SI, selectivity index (CC_{50}/EC_{50}).
doi:10.1371/journal.pone.0048685.t002

Effect of C-29EA on NS3 Protease Activity

Serine protease and helicase domains are respectively located on the N-terminal and C-terminal portions of NS3 [32]. Thus, we examined the effect of C-29EA on NS3 protease activity by using an NS3 protease assay based on FRET. NS3/4A serine protease was mixed with various concentrations of C-29EA. The initial velocity at each concentration of C-29EA was calculated during a 120 min reaction. The initial velocity in the absence of C-29EA represented 100% of relative protease activity. C-29EA decreased the serine protease activity in a dose-dependent manner (Fig. 7). The IC_{50} of C-29EA was 10.9 μg/ml, which is similar to the value estimated by helicase assay. These results suggest that C-29EA includes the compound(s) inhibiting the protease activity of NS3 in addition to the helicase activity.

Combination Antiviral Activity of C-29EA and Interferon-alpha

Treatment with C-29EA may potentiate inhibitory action of interferon-alpha, since it inhibited the protease and helicase activities of NS3 but not induce the interferon response as described above. Then, we examined effect of treatment using both interferon and C-29EA on HCV replication. The replication

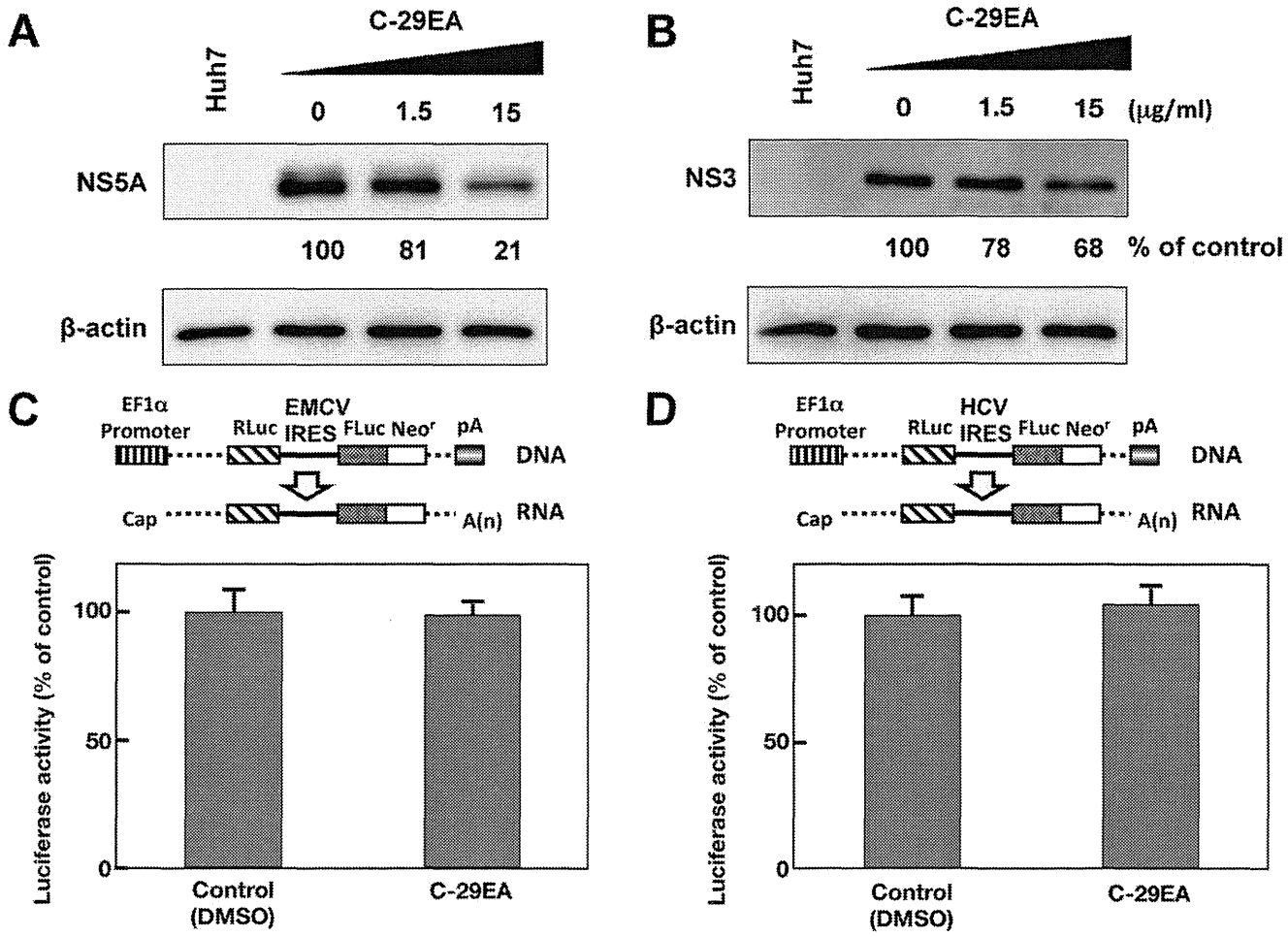

Figure 3. Effect of C-29EA on expression of viral proteins in replicon cell lines. The Huh7 replicon cell lines derived from genotype 1b (A) and 2a (B) were incubated with C-29EA at 37°C for 72 h. The treated cells were harvested and then subjected to Western blotting. Treatment with DMSO corresponds to '0'. The bicistronic gene is transcribed under the control of the elongation factor 1α (EF1α) promoter. The upstream cistron encoding *Renilla* luciferase (RLuc) is translated by a cap-dependent mechanism. The downstream cistron encodes the fusion protein (Feo), which consists of the firefly luciferase (Fluc) and neomycin phosphotransferase (Neo^r), and is translated under the control of the EMCV IRES (C) or HCV IRES (D). The Huh7 cell line transfected with the plasmid (each above the panel in C and D) was established in the presence of G418. The cells were incubated for 72 h without (control) and with 15 μg/ml of C-29EA. Firefly or *Renilla* luciferase activity was measured by the method described in Materials and Methods and was normalized by the protein concentration. F/R: relative ratio of firefly luciferase activity to *Renilla* luciferase activity. F/R is presented as a percentage of the control condition. Error bars indicate standard deviation. The data represent three independent experiments.
doi:10.1371/journal.pone.0048685.g003